

1 SOE THURA TUN & WATKINSON, I. M. 2016. The Sagaing Fault. *In*: BARBER, A. J., RIDD, M. F., KHIN
 2 ZAW & RANGIN, C. (eds.) *Myanmar: Geology, Resources and Tectonics*. Geological Society, London,
 3 Memoir.

4 The Sagaing Fault

5 SOE THURA TUN¹ & IAN M. WATKINSON^{2*}

6
 7 ¹*Myanmar Earthquake Committee, Myanmar Engineering Society Building,*

8 *Hlaing Universities Campus, Yangon, Myanmar*

9 ²*Department of Earth Sciences,*

10 *Royal Holloway University of London, Egham, Surrey TW20 0EX, United Kingdom*

11 *Corresponding author (e-mail: ian.watkinson@rhul.ac.uk)

12

Text words	15,888
References number (words)	163 (4,831)
Tables words	0
Figures number	15

13 **Abbreviated title:** Sagaing Fault

14 The Sagaing Fault is amongst the longest and most active strike-slip faults in the world (e.g. Molnar
 15 & Dayem 2010; Robinson *et al.* 2010; Searle & Morley 2011). It accommodates more than half of the
 16 right-lateral motion between Sundaland and India, within the diffuse plate boundary along the eastern
 17 margin of India, which occupies much of Myanmar (e.g. Vigny *et al.* 2003; Nielsen *et al.* 2004;
 18 Socquet *et al.* 2006) (Fig. 1). Acting as a ridge-subduction transform (Le Dain *et al.* 1984; Guzmán-
 19 Speziale & Ni 1996; Yeats *et al.* 1997), the 1500 km long Sagaing Fault links major thrust systems in
 20 the north, such as the Naga, Lohit and Main Central thrust zones near the eastern Himalayan syntaxis,
 21 to the Andaman Sea spreading centre in the south (e.g. Win Swe 1970; Le Dain *et al.* 1984; Guzmán-
 22 Speziale & Ni 1993; Curray 2005). Acting as a sliver-bounding lithospheric strike-slip partition
 23 inboard of a 3700 km long section of oblique subduction at the Sunda Trench, it links to the dextral
 24 West Andaman and Sumatran faults in the south (e.g. Curray *et al.* 1979; Nielsen *et al.* 2004; Curray
 25 2005; Searle & Morley 2011).

26 Topographic scarps, lineaments, earthquake clusters and gravity anomalies along the trace of the
 27 Sagaing Fault have long been recognised as indicating the presence of an important N-S trending
 28 structure west of the Shan Plateau (e.g. La Touché 1913; Coggin Brown & Leicester 1933; Chhibber
 29 1934; Dey 1968; Aung Khin *et al.* 1970) (Fig. 2a). Large parts of the fault were first documented and
 30 pressure ridges, sag ponds and right-lateral offsets interpreted as signals of a major strike-slip fault by
 31 Win Swe (1970, 1972), who also introduced the name *Sagaing Fault*. Further research during the last
 32 two decades has begun to reveal the fault's profound role in the tectonic evolution of south and
 33 southeast Asia (e.g. Bertrand *et al.* 2001; Vigny *et al.* 2003), and the great hazard it poses to the
 34 millions who live along its trace (e.g. Hurukawa & Phyo Maung Maung 2011; Wang *et al.* 2011).

35 **Tectonic setting**

36 Myanmar straddles the complex oblique plate boundary between the India-Australia plate and
37 Sundaland, the SE promontory of Eurasia (e.g. Hall & Morley 2004; Nielsen *et al.* 2004; Curray
38 2005; Kundu & Gahalaut 2012) (Fig. 1). The Sunda trench and arc, related to the down-going Indian
39 plate, become progressively more parallel to Indian plate motion northwards past Sumatra and into the
40 Indo-Myanmar ranges (e.g. Nielsen *et al.* 2004; Whittaker *et al.* 2007). In the south, simple strain
41 partitioning between the Sumatra trench and the Sumatran Fault (e.g. McCaffrey 1996) gives way to a
42 wide zone of distributed deformation in Myanmar between the Andaman Sea and the eastern
43 Himalayan syntaxis in the north (e.g. Vigny *et al.* 2003; Nielsen *et al.* 2004; Sahu *et al.* 2006).
44 Contraction is accommodated in the Indo-Myanmar ranges in the west, while 18-20 mm/yr of a total
45 of 35 mm/yr right lateral motion between India and Sundaland is partitioned onto the Sagaing Fault,
46 with the remainder distributed across dextral structures within the Indo-Myanmar ranges and far
47 inboard of the trench (e.g. Molnar & Tapponnier 1975; Curray *et al.* 1979; Tapponnier *et al.* 1982; Le
48 Dain *et al.* 1984; Mitchell 1993; Vigny *et al.* 2003). The Sagaing Fault thus defines the western
49 margin of Sundaland and the eastern margin of the Neogene Burma Plate, a fore arc sliver which
50 occupies much of western Myanmar, is partially coupled to the Indian plate, and is bounded by active
51 tectonic structures (Curray *et al.* 1979).

52 Conversely, the Sagaing Fault lies close to but does not mark the western margin of the Gondwana-
53 derived Sibumasu continental block which underlies eastern Myanmar (Ridd 1971; Bunopas 1981;
54 Metcalfe 1984). The western margin of that block in Myanmar is marked at the Shan Scarp by the
55 Mogok Metamorphic Belt (e.g. Searle & Ba Than Haq 1964; Mitchell *et al.* 2007) (Fig. 2b), and the
56 Slate Belt - a sliver of late Palaeozoic glacial marine pebbly mudstones that comprise the Karen-
57 Tenasserim Unit of Bender (1983) or the Mergui Group of Mitchell *et al.* (2002, 2007) that may have
58 been thrust onto the Sibumasu margin in the Late Triassic to Early Jurassic (Mitchell 1992) or
59 translated by a system of dextral faults east of the present-day Sagaing Fault during the Late
60 Cretaceous to Paleogene (Ridd & Watkinson 2013). It remains unclear how far such continental
61 basement continues west of the Sagaing Fault, where it is mostly buried below thick siliciclastic
62 sequences of the Myanmar Central Basin (e.g. Stephenson & Marshall 1984; Pivnik *et al.* 1998; Win
63 Swe 2012).

64 West of the metamorphics along the margin of Sibumasu, the basement is poorly known. A West
65 Burma block (which is not the same as the Sagaing Fault-bounded Neogene Burma Plate) has been
66 interpreted as an island arc thrust onto the western margin of SE Asia during the Middle Jurassic
67 (Mitchell 1981) or Late Cretaceous to Eocene (e.g. Mitchell 1992, 1993). The same block has also
68 been viewed as a fragment of Sibumasu separated in the Triassic and re-accreted during the Early
69 Cretaceous (e.g. Hutchinson 1989), a tectonic slice of the Indochina terrane translated during the
70 Triassic to the western margin of Sibumasu (e.g. Barber & Crow 2009), or an Australian fragment that
71 collided with Sibumasu in the Early Cretaceous (Metcalfe 1996) or Late Cretaceous to Eocene (e.g.
72 Charusiri *et al.* 1993; Hutchison 1994). However, recent work on the provenance of detrital zircons
73 within Triassic turbidites in western Myanmar suggests that West Burma was in place alongside SE
74 Asia before the Mesozoic (Sevastjanova *et al.* 2015), or that Sibumasu extends westwards to the
75 Western Ophiolite Belt suture (Gardiner *et al.* 2015).

76 The Sagaing Fault is closely associated with a number of Cenozoic structures within central Myanmar
77 (Fig. 2a). Many of these structures remain active (e.g. Coggin Brown 1917; Wang *et al.* 2014), yet
78 many probably pre-date the Sagaing Fault and may have played a role in the Neogene to Recent
79 evolution of the fault (e.g. Morley 2012).

80 Immediately east of the Sagaing Fault between Mandalay and the Gulf of Mottama, the Shan Scarp
81 fault zone forms the prominent eastern topographic margin of the Shan Plateau and appears to be
82 obliquely truncated by the Sagaing Fault (Bertrand & Rangin 2003) at about 23°N. Composed of a
83 post-Middle/Upper Miocene dextral transpressional fold and thrust belt trending 140°-160°, the Shan
84 Scarp fault zone places pre-Cenozoic rocks of the Shan Plateau over Mogok Metamorphic Belt
85 gneisses at the margin of the Central Basin (Bertrand & Rangin 2003) (Fig. 2b). The southernmost
86 segment of the fault zone includes the Panlaung and Taungoo faults which bound the Phuket Slate
87 Belt and may have their origins as early Paleogene strike-slip splays of the Mae Ping Fault (e.g.
88 Garson *et al.* 1976; Morley 2004; Ridd & Watkinson 2013).

89 Lying between the Sagaing Fault and the Shan Scarp fault zone, the Mogok Metamorphic Belt
90 comprises a narrow strip of gneisses and schists which in the north curves around the Bhamo Basin,
91 and may be continuous with northern Thailand metamorphic core complexes such as Doi Suthep and
92 Doi Inthanon, and the Lhasa terrane in south Tibet (Mitchell 1993; Mitchell *et al.* 2007, 2012; Searle
93 *et al.* 2007). Like other areas close to the India-Asia suture (e.g. Karakoram/Lhasa/Qiangtang blocks),
94 the Mogok Metamorphic Belt experienced Late Cretaceous pre-collisional magmatic thickening,
95 Paleogene post-collisional thickening, followed by high temperature metamorphism and leucogranitic
96 melting (Barley *et al.* 2003; Searle *et al.* 2007). An early phase of metamorphism is sealed by ~59 Ma
97 dykes, followed by high temperature Eocene-Oligocene metamorphism from 37 Ma (possibly even 47
98 Ma) to 29 Ma, and all metamorphic fabrics are sealed by 24.5 Ma ± 0.3 Ma leucogranites (Searle *et al.*
99 *et al.* 2007). Gently plunging ductile stretching lineations representing NNW-SSE orientated
100 transtension overprint older fabrics, and yield mica Ar-Ar plateaux from 27-25 Ma in the south to
101 22.7-16.6 Ma in the north (Bertrand *et al.* 1999; 2001). Apatite fission track ages range from 18.7-
102 14.6 Ma (Torres *et al.* 1997), supporting a period of Late Oligocene-Mid-Miocene cooling and
103 exhumation.

104 East of the Shan Scarp fault zone is the N-S trending dextral Kyaukkyan Fault, which passes through
105 the Inle Lake pull-apart system and curves into the NW-SE trending Mae Ping Fault in the southeast
106 (Soe Min *et al. this volume*). The Kyaukkyan Fault produced perhaps the largest recorded earthquake
107 in Myanmar (M_w 8.0 (Gutenberg & Richter, 1954)) centred near Pyin-Oo-Lwin in 1912 (Coggin
108 Brown 1917), though it has generated little seismicity since then. Like the presently dextral Mae Ping
109 Fault in Thailand (Lacassin *et al.* 1997), the Kyaukkyan Fault shows evidence of slip sense reversal
110 after an earlier phase of sinistral activity (Wang *et al.* 2014), which may indicate that it, like the Mae
111 Ping Fault, is a longer-lived structure than the continuously dextral Sagaing Fault.

112 Near the northern termination of the Kyaukkyan Fault east of Mogok, a series of apparently left-
113 lateral faults, including the Kyaukme and Momeik (*Nanting* in China) faults, trend ENE-WSW and
114 terminate adjacent to the Sagaing Fault near Thabeikkyin. These arcuate faults, like the parallel Nam
115 Ma Fault further east which generated the 2011 M_w 6.8 Tarlay earthquake, are part of the broad Shan
116 fault system (Soe Thura Tun *et al.* 2014), which may partially accommodate clockwise flow of
117 continental crust around the eastern Himalayan syntaxis (e.g. Royden 1996; Copley & McKenzie
118 2007). The faults' orientations are broadly related to GPS vectors in a stable Eurasia reference frame
119 (e.g. Niu *et al.* 2005). Correspondingly the most northerly members of this fault population, such as
120 the Ruili Fault, attain a more NE-SW trend and become sub-parallel to the termination splays of the
121 Sagaing Fault on the far side of the Bhamo Basin, though their sense of displacement is opposite.

122 Occupying the 200 km wide valley between the Shan Scarp in the east and the Indo-Myanmar ranges
123 in the west, the Myanmar Central Basin represents a postulated fore-arc/back-arc basin filled largely
124 with Cenozoic shallow marine and terrestrial sediments, with major depocentres bounded in the east

125 by the Sagaing Fault (e.g. Pivnik *et al.* 1998). The basin's linked *en echelon* sub-basins include (from
126 north to south): the Hukawng, Chindwin, Bhamo, Salin and Prome basins, which record NNW-SSE
127 directed extension (Pivnik *et al.* 1998) coeval with fabrics recording ductile transtension in the Mogok
128 Metamorphic Belt (Bertrand & Rangin 2003). The basin also contains calc-alkaline andesite-dacite
129 volcanics related to east-dipping subduction below the basin, that had likely ceased by Mid-Miocene
130 times (e.g. Lee *et al.* 2010; Searle & Morley 2011; Gardiner *et al.* 2015). Late Miocene-Recent basin
131 inversion resulted in reactivation of the extensional faults, and development of a series of NNW-SSE-
132 trending *en echelon* folds within the basin (e.g. Pivnik *et al.* 1998; Rangin *et al.* 1999). One prominent
133 area of inversion-related uplift is Pegu Yoma, hilly terrain stretching from Bago (formerly *Pegu*) in
134 the south almost to Sagaing in the north. It is bounded in the east by linear segments of the Sagaing
135 Fault. Along its western margin thrusts such as the West Pegu Yoma and Gwecho faults (Soe Thura
136 Tun & Maung Thein 2012) are part of a suite of *en echelon* thrusts and associated hangingwall
137 anticlines that occupy the low relief western half of the basin. The modern Ayeyarwaddy River passes
138 around the north and west of Pegu Yoma, and appears to have been diverted from an original route
139 along the southern Sagaing Fault (now occupied by the Sittaung River) by uplift of the hills.
140 Bounding structures along the west side of the Central Basin include dextral strike-slip, oblique and
141 thrust faults such as the Seindaung, Kabaw and East Limb faults (e.g. Hla Maung 1987; Searle &
142 Morley 2011; Wang *et al.* 2014).

143 **Tectonic geomorphology**

144 For much of its onshore length the Sagaing Fault passes through low topography west of the Shan
145 Scarp. Unlike the sinuous Shan Scarp fault zone across which the ground rises over 1 km in a short
146 distance, the Sagaing Fault is expressed by more subtle but highly linear topographic features that are
147 only sometimes associated with significant topographic relief (e.g. Dey 1968; Le Dain *et al.* 1984).
148 Major geomorphic domains of the Sagaing Fault comprise the Sittaung/Ayeyarwaddy deltas in the
149 south, the eastern scarp of Pegu Yoma, the palaeo-Ayeyarwaddy valley, the modern Ayeyarwaddy
150 valley and the northern Basin and Range topographic domain (Fig. 3).

151 Overlapping deltas of the Sittaung, Ayeyarwaddy and Bago rivers, which rise to elevations rarely
152 greater than 10 m, are crossed by networks of meandering rivers, abandoned channels and ox-bow
153 lakes. Frequent avulsions combined with intense agricultural activity mostly erase evidence of active
154 faulting. On the delta top south of Bago, several low linear pressure ridges (<40 m elevation) lie along
155 the 1-2 km wide zone between the Sagaing Fault and a parallel strand, the Pale Fault (Tsutsumi &
156 Sato 2009) (Fig. 4a). Elsewhere along the Bago segment the fault is marked by remarkably straight
157 geomorphic lineaments defined by small linear sag ponds and changes in soil moisture and vegetation
158 several tens of metres either side of the fault (Fig. 5a). In places, soil is anomalously moist (dark
159 colour, solid deep green vegetation, lines of trees), reflecting springs or poorly drained sag ponds
160 filled with lacustrine deposits; or it is anomalously well drained (light mottled colour, patchy
161 vegetation), a result of accumulated coseismic sand blows or sandy sag pond fill. In the area around
162 Bago, fault scarps up to 2.8 m high lie along the trend of several low ridges and sag ponds. Streams,
163 terrace risers, rice paddy dikes, property boundaries, and a wall show right-lateral offsets of up to 18.6
164 \pm 0.5 m, accumulated during several historic earthquakes, including the May 1930 M_w 7.2 event
165 (Tsutsumi & Sato 2009).

166 The eastern scarp of Pegu Yoma along the Pyu segment is where the Sagaing Fault has its clearest and
167 most simple geomorphic expression (Fig. 5b). The scarp rises almost 450 m above the Sittaung valley
168 in the east, is highly linear and is crossed by numerous streams displaying right-lateral offset. This

169 section was first compared to the San Andreas Fault in California by Dey (1968), and the stream
170 offsets are as regular and well defined as they are along the famous Carrizo Plain section of the San
171 Andreas Fault (e.g. Wallace 1968). A bajada of broad, low amplitude stream-flow-dominated alluvial
172 fans flanks the ridge, with the traces of palaeochannels clearly radiating from the stream source and
173 fan axes offset from the upstream incised stream. Very poorly developed triangular facets mark the
174 most linear sections of the scarp. In a number of places, notably NNW of Pyu, strips of the bajada are
175 uplifted >20 m adjacent to the fault, possibly by west-dipping reverse faults (Replumaz 1999). Incised
176 streams crossing the uplift occupy rounded, well vegetated gulleys, and larger rivers occupy wide
177 meander belts, suggesting that the uplift is either very slow or not presently active. Dextral river
178 offsets are well developed across the strike-slip segment, but not across the easterly reverse faults,
179 suggesting complete strain partitioning.

180 East of Meiktila the Sagaing Fault lies in flat topography of the palaeo-Ayeyarwaddy valley. A north-
181 plunging anticline alongside the fault at 20.4°N (Fig. 4b) near the northern limit of Pegu Yoma is
182 defined by relatively subtle topographic relief (~50 m). It lies at a gentle southward change in fault
183 trend from nearly N-S to NNW-SSE. The surface fault trace is highly segmented and sag ponds exist
184 at three right-step-overs no more than 0.5 km wide. A network of wide, meandering river channels
185 draining east from the fold axis are beheaded close to the fault trace, and are marked by darker, less
186 mottled farmland than surrounding areas. All the wide channels terminate at the fold, having
187 presumably been isolated from their upstream basins by growth of the fold. Deeply incised modern
188 tributaries on the eastern fold limb are offset to the right as they cross the fault. Abandoned meander
189 bends along the top of the fold indicate progressive northward fold propagation and deflection of the
190 river around the fold tip, clearly supporting young (Holocene?) dextral transpression along the
191 Sagaing Fault.

192 The Ayeyarwaddy River flows along or parallel to the Sagaing Fault for 180 km from Tagaung to
193 Sagaing city. The sediment-laden river occupies a sprawling system up to 10 km wide of braided
194 channels along the southern reach of this section, bounded in the west by the Sagaing Fault. The river
195 is briefly deflected west of the fault trace by Pleistocene basalts north of Singu (Bertrand *et al.* 1998).
196 The river's northern reach is a remarkably linear single channel rarely more than 1 km wide
197 dominated by erosion and bounded by linear fault-controlled topographic ridges. Steep-sided slopes,
198 triangular facets, (Fig. 4c) offset streams and deltas and down-cutting into Recent fluvial sands
199 characterise this reach. Two dry streams offset ~1.7-2.0 m near Thabeikkyin (Fig. 4d) include ~0.78 m
200 of local dextral displacement acquired during the 2012 M_w 6.8 earthquake, leaving 0.9-1.2 m which
201 can be attributed to a previous event, possibly the 1946 M_w 7.7 Wuntho earthquake. The linear
202 morphology of sand bars cut by recent Sagaing Fault activity in the Ayeyarwaddy River at Sabeanago
203 (Fig. 5c) reveal rapid along-strike changes in uplift/subsidence, a characteristic of strike-slip faulting.
204 Immediately south of a downthrown western block defining the modern river channel, the fault comes
205 onshore and is bounded in the west by Thein Taung ridge, where folded Neogene sandstones are
206 uplifted. Similar pressure ridges can be seen at a variety of stages of development along the
207 Ayeyarwaddy domain. While not quite fractal, there is an element of self-similarity in the morphology
208 of different sized ridges. At the smallest scale, embryonic ridges up to 0.5 m high in agricultural soils
209 deformed by the 2012 Thabeikkyin earthquake are bounded by a segmented strike-slip system on one
210 side, and an upwards flattening reverse fault on the other (Fig. 6a). A longer-lived pressure ridge in
211 Quaternary fluvial/lacustrine sediments (Fig. 6b) is 1.5 m high, has a length:width ratio of about 3:1,
212 and is again bounded on one side (east) by a strike-slip fault. Ridges north of Singu up to 25 m high
213 are bounded by transpressional strike-slip systems, exhume gently folded Irrawaddy Group sands
214 (Fig. 6c) and are locally capped by vesicular Singu basalt. An asymmetric shutter ridge exhuming

215 highly tectonised amphibolites north of the Singu basalt plateau is >100 m high (Fig. 6d), and has
 216 over-steepened slopes scarred by landslides on the side bounded by the Sagaing Fault. A slightly
 217 higher but highly elongate ridge parallel to the Ayeyarwaddy river is bounded on both sides by strike-
 218 slip fault strands and has an almost symmetric topographic cross-section (Fig. 6e). All of these ridges'
 219 long axes are either sub-parallel to the local Sagaing Fault trend, or are orientated <5° anticlockwise.
 220 Where close together they are arranged *en echelon*.

221 The most prominent pressure ridge, Sagaing Ridge (Fig. 6f), rises 330 m above the adjacent braided
 222 Ayeyarwaddy River, and is flanked by alluvial fans on its western side (e.g. Myint Thein *this volume*).
 223 Sagaing Ridge tapers in the north to a slightly elevated flat-topped plateau. Large antecedent streams
 224 flowing right across the plateau from west to east are deeply incised into the plateau. Smaller east
 225 flowing streams originating on the plateau top represent modern drainage, and are characterised by
 226 steep-sided canyons, slope failures and deltas where the streams enter the Ayeyarwaddy, indicating
 227 energetic down-cutting as a result of recent uplift. The highly linear western margin of Sagaing Ridge
 228 is marked by poorly developed triangular facets. A smaller, parallel ridge, Minwun Ridge, lies to the
 229 west of the main fault strand. In the valley between the two ridges is Yega In, a linear lake which may
 230 be a pull-apart basin, and a number of elongate sag ponds filled with wet, fine grained sediments. In
 231 the valley immediately north of Sagaing city, a 1 m high west-facing, partly collapsed scarp cuts
 232 across an embayment in the mountain front and may represent surface rupture and subsidence during
 233 a historic earthquake (Fig. 4e). The eastern margin of Sagaing Ridge is more sinuous, perhaps because
 234 bounding faults are less active, more segmented or dip at a shallower angle.

235 North of the point where the Ayeyarwaddy River is captured by the Sagaing Fault valley (at about
 236 23.5°N), splays of the Sagaing Fault partly define a series of prominent, steep-sided curvilinear ranges
 237 separated by basins of approximately equal width (Fig. 7). Elevations range from about 107 m in the
 238 basins (e.g. Indaw Lake) to over 1400 m in the ranges. Ranges are bounded on one or both sides by
 239 basin-dipping faults which are in some cases marked by triangular facets and flanked by alluvial fans.
 240 In many cases modern axial drainage within the basins is asymmetric, suggesting tilting of the basin
 241 floor towards the active fault. Such normal faulting and topography has similarities to regions of
 242 extreme continental extension, for example basin and range domains of the western North American
 243 Cordillera, central Turkey, south Tibet and northern Thailand, all regions of hot crust, crustal
 244 thickening, uplift, collapse and extension (e.g. Coney & Harms 1984; Armijo *et al.* 1986; Wernicke
 245 *et al.* 1987; Rhodes *et al.* 2005; Genç & Yürür 2010; Whitney *et al.* 2013). However, the apparent
 246 localisation of modern tectonic activity along only one fault strand (e.g. Maurin *et al.* 2010) and the
 247 presence of higher topography in the west, north and east beyond the region of prominent basins and
 248 ranges indicates that the northern Sagaing Fault area is not a typical 'basin and range' region.

249 **Segmentation**

250 The Sagaing Fault is distinguished from other major strike-slip faults of similar length, such as the
 251 Sumatran Fault and the Altyn Tagh Fault, by its straightness and apparent structural continuity (e.g.
 252 Vigny *et al.* 2003). Straight and continuous faults can result from the removal of complexities such as
 253 step-overs and rotation of pre-existing fabrics into parallelism with the through-going fault by high
 254 cumulative displacements (e.g. Wesnousky 1988; Stirling *et al.* 1996; King & Wesnousky 2007). The
 255 range of high displacement estimates for the Sagaing Fault, ranging from 100-150 km (Bertrand &
 256 Rangin 2003) to 460 km (Curry *et al.* 1979; Hla Maung 1987) and even 700 km (Replumaz &
 257 Tapponnier 2003), support the conclusion that the Sagaing Fault has experienced considerable strain
 258 smoothing. In contrast, the similar length North Anatolian Fault is highly segmented and possesses

259 several wide rupture-arresting restraining and releasing step-overs along its length (e.g. Lettis *et al.*
260 2002; Duman *et al.* 2005). Estimates of its displacement (25-85 km, e.g. Armijo *et al.* 1999) are up to
261 an order of magnitude less than those proposed for the Sagaing Fault, which are discussed in the next
262 section.

263 Significant step-overs and bends along the central 700 km section of the Sagaing Fault are poorly
264 documented, if they exist at all. Hurukawa and Phyo Maung Maung (2011) suggested that the Sagaing
265 Fault is segmented based on the occurrence of M6 events at the termini of M7 earthquake-generating
266 segments. Small sag ponds and pressure ridges along the fault are common (e.g. Dey 1968; Tsutsumi
267 & Sato 2009) (Fig. 6), though it is unclear whether even the largest pressure ridge, Sagaing Ridge, can
268 be related to extant fault complexities, or has simply been translated along the fault from a
269 subsequently breached transpressive feature. Interpretation of satellite imagery suggests that step-
270 overs >3-5 km wide do not currently exist, and Robinson *et al.* (2010) consider that the central
271 Sagaing Fault entirely lacks steps wider than 1 km.

272 Here we describe Sagaing Fault segments based on interpretation of 30 m ASTER GDEM satellite
273 data, the ESRI World Imagery compilation, which includes 2.5 m SPOT and <1 m DigitalGlobe
274 imagery, and field observation of the fault. The fault interpretation incorporates previous mapping,
275 including Tsutsumi and Sato (2009), Soe Thura Tun and Maung Thein (2012) and Wang *et al.* (2014).
276 Numerous schemes have been proposed to divide the Sagaing Fault into structurally distinct
277 segments, a task complicated by the remarkable continuity of the central 700 km from 17-23° N (e.g.
278 Vigny *et al.* 2003). Wang *et al.* (2014) divided the onshore Sagaing Fault into five main segments,
279 plus seven additional segments within four active strands of the northern horsetail array, based on
280 fault geometry, geomorphic expression and historical seismicity. Here we broadly follow the work of
281 those authors, modified based on new satellite imagery interpretation and field observations (Fig. 2a
282 & 7).

283 *Northern segments and strike-slip termination*

284 Strike-slip along the Sagaing Fault terminates in a northern sickle-shaped horsetail splay largely
285 within Kachin State, comprising a paired right and left bend system almost 500 km from north to
286 south (Fig. 7). The sickle-shaped geometry is influenced by clockwise flow of the lower crust around
287 the eastern Himalayan syntaxis (e.g. Royden 1996; Copley & McKenzie 2007; Rangin *et al.* 2013).
288 Within this splay dextral strike-slip is transferred via a basin and range-style region of linear fault-
289 bounded basins and high ranges, such as the Katha-Gangaw range, exposing mid- and lower-crustal
290 units, to compressional structures around the eastern Himalayan syntaxis. As such the northern
291 horsetail splay is presently not strictly a termination splay, rather a splaying zone of strain transfer
292 converting strike-slip to extension at the releasing bend in the region of Myitkyina, and contraction at
293 the restraining bend in the region of Putao and beyond. The development of the present-day releasing
294 segments may be a consequence of rotation of earlier straight fault segments by gravitational collapse
295 of the Tibet Plateau (Rangin *et al.* 2013).

296 The major northern splay is composed of three (Maurin *et al.* 2010) or four (Wang *et al.* 2014) main
297 splay systems. Excluding the minor splays that originate at Singu (see below) the most westerly splay
298 is composed of the section of the Sagaing segment north of the prominent Ayeyarwaddy River bend,
299 termed Tawma segment by Wang *et al.* (2014). The Tawma segment steps to the left, via a series of *en*
300 *echelon* faults, to the Ban Mauk segment in the northwest, which itself terminates in a prominent
301 releasing horsetail splay east of Taungthonton volcano (Fig. 8a). Although the Ban Mauk segment

302 occupies a deeply incised narrow valley, geomorphology suggests that the segment has a low rate of
303 Quaternary slip (Wang *et al.* 2014).

304 The Indaw and Mawlu segments make up a complex zone of faulting that terminates in the south
305 close to the tips of the Tawma and Sagaing segments. This zone forms the western margin of the
306 Katha-Gangaw belt, a >1300 m high curvilinear range of mountains composed of low-medium
307 pressure – high temperature gneisses which pass east into lower grade metamorphic rocks of the
308 Tagaung-Myitkyina belt and the Mogok Metamorphic Belt on the east side of the Bhamo Basin
309 (Mitchell *et al.* 2007; Searle *et al.* 2007). Indaw lake lies at a right step between the Indaw segment
310 and Mawlu segment (Fig. 8b). The rhomboidal step-over is 10 km long and almost 3 km wide, a 3:1
311 length:width ratio characteristic of many pull-apart basins. Satellite imagery reveals evidence of
312 recent normal faulting in the alluvial and lacustrine sediments of the basin, including sets of inward-
313 dipping NE-SW trending normal faults linking sidewall fault systems. Although the lake itself forms
314 the locus of local subsidence at the step-over, the modern depocentre and axial drainage lies near the
315 western edge of the 80 km long basin west of the fault segments. Nonetheless, up to 4 km of dextral
316 geomorphological offset (Wang *et al.* 2014) and ~18 mm/yr of dextral slip measured using GPS
317 across the Kaimang segment along strike to the north (Maurin *et al.* 2010) indicate that these
318 segments comprise perhaps the most active of the Sagaing Fault's northern splays.

319 The horsetail splay proper originates from the northern tip of the Mawlu segment, where Indawgyi
320 lake lies at the intersection of the Mawlu, Shaduzup and Kamaing segments, as well as a number of
321 other minor branching structures (Fig. 8c). Unlike the Shaduzup segment, the Kamaing segment,
322 which includes strands locally known as the Takri and Koma faults, shows geomorphic evidence of
323 recent activity and continues around the Hukawng basin towards the Assam Valley in India (Wang *et al.*
324 2014). This is also the segment across which Maurin *et al.* (2010) measured all instantaneous
325 strain, with other strands of the splay inferred to be presently inactive. Like Indaw Lake, the larger
326 Indawgyi Lake has been interpreted as forming at a releasing step-over (e.g. Soe Thura Tun 1999; Hla
327 Hla Aung 2011), with normal faults concentrated in its NW and SE quadrants, though its position at
328 the intersection of several fault segments makes its structural architecture unclear. It may be related to
329 the right-step and linkage between the northern Ban Mauk horsetail splay and the southern Shaduzup
330 segment tip, or a narrower step-over between the Mawlu and Kamaing/Shaduzup segments. A third
331 option involves strands of the Mawlu segment passing below alluvial fans south of the lake, and
332 linking directly with the Kamaing segment. This would lend the lake a releasing bend geometry. Like
333 Indaw, Indawgyi has a length:width ratio of 3:1, and like the extremely shallow Inle Lake on the Shan
334 Plateau, Indawgyi's 22 m depth is anomalously shallow for a pull-apart lake – reflecting either slow
335 tectonics or rapid sedimentation. Oral reports suggest that Indawgyi lake formed in historic times:
336 several thousand *Taman* (an early tribe living in the upper Chindwin region) reportedly died when the
337 previously dry and fertile Indawgyi valley was catastrophically flooded (Grant Brown 1911). No date
338 for this event or record of an earthquake is reported, and it remains unclear whether the flooding of
339 Indawgyi was the result of massive coseismic subsidence or a landslide.

340 Forming the easternmost segment of the Sagaing Fault horsetail splay, the Mogang segment forms the
341 northern margin of the Bhamo basin, and links to the Sagaing-Namyin Fault before terminating in a
342 north-directed thrust near Putao. The Mogang segment forms the western margin of the narrow belt of
343 structures and exhumed metamorphic complexes of northernmost Sundaland in Yunnan, which
344 include the Gaoligong Shan and Chong Shan shear zones, the Diangcan Shan and Ailao Shan-Red
345 River Fault (e.g. Socquet & Pubellier 2005; Searle & Morley 2011). Despite evidence of a 10 km river
346 offset, the Mogang segment is presently seismically quiet (Wang *et al.* 2014) and does not show a
347 significant geodetic slip rate (Maurin *et al.* 2010).

348 *Sagaing segment*

349 The Sagaing segment, immediately south of the termination splay (Fig. 2a), is interpreted by Wang *et al.* (2014) to originate close to the convergence of the northern termination splay at a left-step-over at
350 23.5°N, and to terminate south of the uplifted pressure ridges close to Sagaing city. We prefer to
351 extend the segment north to about 23.9°N on the basis of 1) scant evidence for the uplift that might be
352 expected at a major left-step; 2) the apparent continuity of the fault trace along the west bank of the
353 Ayeyarwaddy River north of Male; 3) the marked discontinuity of active segments on the east bank
354 north of Sabenago; and 4) a series of left-stepping *en echelon* faults at the tip of the segment north of
355 23.9°N (SW margin of the Indaw basin). This brings the length of the Sagaing segment to >220 km.
356

357 For much of the northern half of the Sagaing segment the Ayeyarwaddy River follows the Sagaing
358 Fault's N-S trace, which also forms the margin of the most westerly extension of the Shan Plateau in
359 the region of soft linkage between the Momeik, Kyaukkyan, Shan Scarp and Sagaing faults. Where
360 the Sagaing Fault forms the plateau margin, a series of small pressure ridges composed of intensely
361 deformed and locally mylonitic paragneisses, mafic rocks and marble, as well as slices of strongly
362 folded Upper Pegu and Irrawaddy clastics mark the fault trace. The ridges are bounded by two sub-
363 parallel fault strands less than 0.5 km apart, with the freshest geomorphic expression on the eastern
364 strand, part of which failed in 2012. A series of narrow sag ponds along the eastern strand reflect
365 shallow segmentation of the Sagaing Fault as it reaches the surface, and include one 40 m wide
366 incipient pull-apart near Thabeikkyin associated with >0.4 m of coseismic subsidence (Fig. 8d). Like
367 Indaw and Indawgyi lakes, the incipient pull-apart lies at a right step-over, has normal faults in its NW
368 and SE quadrants, and an element of dip-slip along the dominantly strike-slip sidewall faults. Unlike
369 the larger basins, the incipient pull-apart represents geologically infinitesimal strain, thus the faults are
370 represented by minor fractures such as R and R' shears, linking P shears and mode I fractures. At
371 higher geologic strain such features become rotated and overprinted by through-going faults, and
372 should not be interpreted on the scale of through-going fault strands (e.g. Christie-Blick & Biddle
373 1985). The fault strands pass north into the Ayeyarwaddy River close to Male, before continuing along
374 the western bank of the river adjacent to a wide region of uplift. Structural control of recent sand bars
375 in the Ayeyarwaddy River between Sabenago and Male (Fig. 5c), supports recent vertical motion
376 along the fault. Wang *et al.* (2014) identify an east facing scarp on a fluvial surface on a less
377 prominent eastern fault trace further north, also indicating recent activity.

378 North of Singu the Sagaing Fault bends and steps to the right and cuts a complex path through the
379 Singu basalt plateau (Fig. 9a), which was emplaced as a 100 m thick series of flows overlying the
380 Mio-Pliocene Irrawaddy Group (e.g. Chhibber 1934; Bender 1983). The potassic alkali trachy-basalts
381 have yielded whole rock ⁴⁰K-⁴⁰Ar ages of 0.45 Ma to 0.25 Ma, and have been displaced 2.7-6.5 km by
382 the Sagaing Fault (Bertrand *et al.* 1998). The fault is expressed through much of the Singu basalt
383 plateau as a discontinuous series of *en echelon* shears with an apparent synthetic Riedel geometry,
384 consistent with lower accumulated strain through the late Pleistocene basalts compared to older rocks
385 elsewhere along the fault zone. Near the south end of the plateau, the fault comprises a multi-strand
386 zone almost 3 km wide on the east Ayeyarwaddy River bank at Kule (Fig. 9a), and passes into an
387 apparently simple trace on the west bank of the river south of Singu town. The partly breached Kule
388 releasing step-over results in graben-like subsidence at Kyet Phyu Taung lake, and likely terminated
389 the November 2012 earthquake surface rupture (see below). This step-over, mid-way along the
390 otherwise continuous Sagaing segment, highlights the difficulty of defining meaningful structural
391 segments. While it arrested the 2012 M_w 6.8 rupture, it appears to have been breached by larger
392 magnitude earthquakes in 1839 and 1946 (Hurukawa & Phyo Maung Maung 2011; Wang *et al.* 2014).

393 West of Singu is the southernmost evidence of splaying into the northern horsetail. Two poorly
394 developed splays, including the Male Fault, curve to the NNW from about 22.5°N before rejoining the
395 main horsetail array at 23.8°N. Though there is little geomorphic evidence of recent activity, both
396 splays truncate folded Mio-Pliocene strata and are associated with small sag ponds.

397 A prominent feature of the southern part of the generally linear Sagaing segment is the presence of
398 several N-S trending pressure ridges, notably Sagaing ridge, whose tectonic geomorphology is
399 described above. Sagaing ridge is bounded by a locally segmented strike-slip fault zone in the west
400 and a system of curved reverse and strike-slip faults in the east (Fig. 9b). The ridge is composed of
401 pelitic gneisses overlain by calcsilicate and marble (De Terra 1943; Myint Thein *et al.* 1982),
402 generally of amphibolite to granulite metamorphic facies, and greenschist facies in Minwun ridge in
403 the west (Kan Saw 1973; Me Me Aung 2007; *both in Myint Thein 2012*). Deformed Miocene to
404 Recent siliciclastic sediments including Upper Pegu and Irrawaddy groups unconformably overlay the
405 metamorphics (Myint Thein *et al.* 1982). Folds and thrusts within these sediments trend along 150°
406 (Bertrand & Rangin 2003). Unlike the young uplift associated with restraining bends along the
407 Meiktila and Nay Pyi Taw segments (see below), the Sagaing ridge uplift does not occur at a local
408 restraining bend or step along the Sagaing Fault. There are a number of alternatives to explain its
409 elevation: 1) it may represent uplift at an older restraining feature subsequently breached and now
410 translated along a straight section of the fault; 2) its position at the apex of the long, gentle westward
411 curve of the onshore Sagaing Fault places it close to the entry point of a regional-scale, albeit very
412 gentle restraining bend (<5°); 3) it may be related to transpression as a result of the westward flow of
413 the Shan Plateau south of the Bhamo Basin, again centred on the apex of the broad westward curve; 4)
414 there may be an element of inselberg amplification whereby the ridge is part of a much larger
415 heterogeneous fault-bounded sliver from which non-crystalline rocks are completely planed away
416 leaving an upstanding metamorphic massif.

417 South of the Ayeyarwaddy River the Sagaing Fault is difficult to trace for about 30 km. However,
418 where the fault can be observed, for example at Mandalay airport, it has stepped to the right of its
419 position at Sagaing city, indicating that the low ground south of the city may result in part from a
420 releasing step/bend up to 4 km wide. This apparent discontinuity forms the intersection between the
421 Sagaing and Meiktila segments, as defined by Wang *et al.* (2014).

422 *Meiktila segment*

423 The northern tip of the Meiktila segment lies close to the Ayeyarwaddy River south of Sagaing city,
424 and the southern tip links to the Nay Pyi Taw basin, making a length of 220 km (Wang *et al.* 2014)
425 (Fig. 2a). From the wide Ayeyarwaddy valley in the north, the segment connects, via a system of
426 actively growing anticlines, to the eastern margin of Pegu Yoma. Gentle restraining double bends at
427 21.2°N and 21.5°N are associated with elongate zones of uplift, while other small ridges may be due
428 to shallow shear dilation in the floodplain sediments (Wang *et al.* 2014). A more pronounced change
429 in orientation along the southern half of the segment, from the nearly N-S Sagaing segment trend to
430 the NNW Nay Pyi Taw trend, is associated with a growing fold at 20.4°N (Fig. 4b), discussed above.
431 Here the surface fault trace is highly segmented and sag ponds exist at three right-step-overs no more
432 than 0.5 km wide. The southern limit of the Meiktila segment is defined by a releasing splay at the
433 northern tip of the rhomboidal Nay Pyi Taw basin. However, an apparently continuous strand of the
434 splay continues south along the Meiktila trend, meaning there is no significant structural break
435 between the Meiktila and Nay Pyi Taw segments.

436 *Nay Pyi Taw segment*

437 The Nay Pyi Taw segment comprises a western strand that includes a paired releasing-restraining
438 double bend system, and a linear cut-off fault along the east side of the Nay Pyi Taw basin which
439 bypasses the bends and is parallel to both the Meiktila and Pyu segments (Figs. 2b & 9c). The two
440 strands are ≤ 11 km apart. Strike-slip strain is distributed across both strands and topographic relief is
441 low (Wang *et al.* 2014). In the north, a releasing double bend forms a 40 km long rhomboidal basin
442 within which lies the newly built capital city Nay Pyi Taw. In the south, a restraining double bend
443 rejoins the main Sagaing Fault trace via a system of splays around the latitude of Taungoo. The
444 restraining double bend is associated with *en echelon* folds within Mio-Pliocene strata of the Upper
445 Pegu and Irrawaddy groups, several of which are truncated by strike-slip fault strands. Alluvial fan
446 uplift east of the southern portion of the cut-off fault is associated with west-dipping reverse faults
447 which continue south to characterise the Pyu segment (Replumaz 1999). Although the Nay Pyi Taw
448 segment is structurally more complex than other central sections of the Sagaing Fault, the apparent
449 continuity of the eastern cut-off fault means that the major releasing and restraining bends need not
450 provide a barrier to rupture propagation along and beyond the segment. From the northern tip of the
451 rhomboidal Nay Pyi Taw basin to the southernmost termination of the restraining bend, the segment is
452 almost 130 km long.

453 *Pyu Segment*

454 The entire, highly linear Pyu segment south of the Nay Pyi Taw restraining bend is orientated about
455 10° anticlockwise from the overall strike of the Sagaing Fault (Wang *et al.* 2014), resulting in
456 characteristic transpression throughout the segment. A prominent restraining step-over at 18°N (Fig
457 9d) produces an elongate zone of uplift immediately east of the main Pegu Yoma ranges, and marks
458 the southern limit of the Pyu segment. Background seismicity at the step-over is high, and it has been
459 interpreted as a low-coupled patch which terminates large seismic ruptures (Wang *et al.* 2011),
460 although the step-over itself is less than 1 km wide, smaller than the minimum empirically determined
461 likely to terminate rupture (e.g. Wesnousky 2006). The northern boundary of the Pyu segment is
462 marked by splays curving west into the Nay Pyi Taw paired bend system. Wang *et al.* (2014) identify
463 splays at 19.1°N near where the 1930 M_w 7.3 Pyu earthquake rupture was arrested, but we prefer to
464 terminate the segment at the most southerly set of splays (Fig. 2a), making the segment only 85 km
465 long and accepting that the 1930 earthquake breached the segment boundary. Strike-slip along the Pyu
466 segment is partitioned onto a highly linear fault at the foot of an east-facing scarp rising >400 m
467 above the Sittaung River basin. An elevated and deeply incised elongate sliver of the basin up to 7 km
468 wide adjacent to the fault may be bounded in the east by west-dipping reverse faults (Replumaz
469 1999).

470 *Bago segment*

471 The Bago segment passes 170 km south from the restraining bend at 18°N to the Mottama Gulf coast
472 (Wang *et al.* 2014) (Fig. 2a). Along large portions of the segment the fault trace is largely obscured
473 because of agricultural activity, recent sedimentation by the Sittaung and Bago rivers and negligible
474 topographic relief. However, geomorphic evidence of earthquakes, including those in 1930 and older,
475 such as fault scarps, subsidence, uplift, offset of streams and field boundaries is well preserved along
476 the segment particularly from Bago south almost to the coast (Tsutsumi & Sato 2009; Wang *et al.*
477 2011). The Pale Fault, a 17 km long fault strand west of and parallel to the main Sagaing Fault, also
478 shows evidence of surface rupture during the 1930 earthquake (Tsutsumi & Sato 2009) and marks a
479 very gentle net right bend in the fault trace. The southernmost 60 km of the onshore fault is
480 remarkably straight and continuous, and trends exactly N-S resulting in no vertical motion. The

481 southern termination of the Bago segment has no structural significance other than being the point
482 where the fault goes offshore, and as such would not be a barrier to rupture propagation.

483 *Southern segments and termination*

484 As it passes offshore into the Gulf of Mottama south of the Bago segment, the Sagaing Fault splays
485 into three segments, two of which terminate in a broad zone of ENE-WSW trending normal faults
486 (Fig. 1). The splays are associated with zones of intense deformation, disruption of the sea floor, and
487 mobilisation of overpressured fluids (Morley 2013), the latter also observed locally onshore, for
488 example at Nay Pyi Taw (Sloan *et al. this volume*), following coseismic liquefaction at Bago
489 (Chhibber 1934) and near Singu (see below). The easternmost splay continues south of the Gulf of
490 Mottama extensional domain to transfer into the Pliocene-Recent Andaman Sea spreading centre and
491 associated transform faults via a series of ENE-WSW trending normal faults (Curry 2005; Morley *et al.*
492 *2011*; Morley 2013). Along strike from the southern tip of the eastern splay, a NNE-trending linear
493 feature interpreted as the ocean-continent boundary offshore the Mergui Archipelago (Curry 2005)
494 may instead be an inactive strike-slip precursor to the modern Sagaing Fault within thinned
495 continental crust, and has been termed the 'South Sagaing' Fault segment by Morley (2013).

496 **Displacement**

497 *Onset of dextral motion*

498 Models for Cenozoic lateral extrusion in response to Indian indentation into Eurasia typically call for
499 substantial dextral shear in the position of the Sagaing Fault and Gaoligong Shan along the western
500 margin of a rigid Indochina block, while the Chong Shan and Ailao Shan-Red River Fault in Yunnan
501 form the sinistral eastern margin of the extruding block (e.g. Tapponnier *et al.* 1982, 1986; Briais *et al.*
502 *1993*; Socquet & Pubellier 2005). However, despite Oligocene and older peak metamorphism and
503 partial melting in Xuelong Shan, Diancang Shan and Ailao Shan metamorphic complexes (e.g.
504 Harrison *et al.* 1992; Zhang & Scharer 1999; Leloup *et al.* 2001), retrograde sinistral shear and
505 exhumation along a discrete Ailao Shan-Red River Fault did not occur until the Miocene (Searle
506 2006). Similarly, there is little evidence for a discrete pre-Mid-Miocene Sagaing Fault, rather a long-
507 lived zone of diffuse dextral shear in Thailand and east/central Myanmar that may have been a lateral
508 extrusion-driven earliest precursor to the localised Recent strike-slip structure (e.g. Le Dain *et al.*
509 1984; Bertrand & Rangin 2003; Socquet & Pubellier 2005; Searle & Morley 2011).

510 At the extreme southern end of the Sagaing Fault, decoupling of West Burma from Sundaland by a
511 zone of diffuse dextral transtension may have its first expression in WNW-ESE directed extension in
512 the Mergui and North Sumatra Basins, which began developing during the Late Eocene to Early
513 Oligocene (Srisuriyon & Morley 2014). Contemporaneous (37-29 Ma) peak high temperature
514 metamorphism in the Mogok Metamorphic Belt close to Mandalay in the north may be associated
515 with NW-SE sinistral transpression along the Mae Ping and Three Pagodas Faults in Thailand (Morley
516 2004; Searle *et al.* 2007; Searle & Morley 2011). These events also shortly follow the 48-40 Ma final
517 phases of diffuse dextral shear and magmatism along the NNE-trending Ranong and Khlong Marui
518 faults on the eastern side of the Mergui Basin in Thailand (Watkinson *et al.* 2011), suggesting a
519 progressive westwards localisation of dextral strain.

520 The NNE-trending 'South Sagaing' Fault segment, along strike from the southern tip of the Sagaing
521 Fault, is parallel to the eastern boundary of the Sewell Rise in the Andaman Sea and bounds a linear
522 Late Oligocene-Early Miocene basin (Morley 2013). If the bounding fault is indeed dextral, this

523 segment could represent the site of the earliest localised strike-slip in the position of the Sagaing
524 Fault.

525 Synchronous with postulated activity along the 'South Sagaing' Fault segment, a diachronous belt of
526 Oligocene to Early Miocene ductile dextral shear overprinted Mogok Metamorphic Belt gneisses and
527 Gaoligong Shan metamorphics in Yunnan (Bertrand & Rangin 2003; Socquet & Pubellier, 2005;
528 Morley 2013), recorded by ductile stretching lineations and northward-younging Ar-Ar cooling ages
529 of 26.9 Ma to 15.8 Ma (Bertrand *et al.* 2001). Ductile extensional fabrics of the Mogok Metamorphic
530 Belt point to a period of post-peak metamorphism transtension which may have included dextral pull-
531 apart basins rooted in the now-exhumed ductile basement (Bertrand & Rangin 2003; Searle *et al.*
532 2007) and extension in the Central Basin (e.g. Bertrand & Rangin 2003). Younger cooling ages of 20-
533 10 Ma further north in the Gaoligong Shan and Chongshan (Wang & Burchfiel 1997; Akciz *et al.*
534 2008; Zhang *et al.* 2012) support uplift by a wave of northward migrating dextral transpression that
535 may have shortly pre-dated Mid to Late Miocene localisation of strain along onshore brittle dextral
536 structures including the Sagaing Fault (Socquet & Pubellier 2005).

537 Ductile fabrics in parts of the central Mogok Metamorphic Belt are sealed by unfoliated Oligo-
538 Miocene syenites and leucogranites (Barley *et al.* 2003; Mitchell *et al.* 2007; Searle *et al.* 2007).
539 Typical of these intrusions, the Sedo syenogranite, which cross-cuts earlier ductile fabrics, yields a
540 SHRIMP age of 22.6 ± 0.4 Ma (Barley *et al.* 2003; Searle *et al.* 2007). Deformation of such Oligo-
541 Miocene intrusions by the brittle Sagaing Fault close to Mandalay supports onset of localised dextral
542 motion along the central part of the fault after 22 Ma (Socquet & Pubellier 2005; Searle *et al.* 2007)
543 and possibly as late as 15 Ma when diffuse dextral strike-slip ceased further east in Thailand (Morley
544 2004; Searle & Morley 2011).

545 In the Andaman Sea the deep Central Andaman Basin spreading centre separates older, rugged
546 bathymetric plateaux of poorly known genesis (Alcock and Sewell Rises, Fig. 1) and forms part of a
547 ~300 km wide right step-over system between the Sagaing Fault and the Sumatran Fault, inboard of
548 the Sunda Trench (e.g. Curray *et al.* 1979; Chamot-Rooke *et al.* 2001; Kamesh Raju *et al.* 2004;
549 Curray 2005; Morley 2013; Srisuriyon & Morley 2014). The Central Andaman Basin lies south of the
550 southern Sagaing Fault termination splay and has a soft linkage with the easternmost strand via a
551 series of ENE-WSW trending normal faults (Morley 2013). The western margin of the spreading
552 centre is similarly marked by dextral faults including the West Andaman Fault zone, which transfer
553 displacement south onto the Sumatran Fault (Kamesh Raju *et al.* 2004; Curray 2005).

554 The spreading centre is inferred to accommodate all residual dextral strain at the tip of the Sagaing
555 Fault, in the same way that the South China Sea has more controversially been inferred to terminate
556 Oligo-Miocene Ailao Shan-Red River Fault sinistral slip (e.g. Tapponnier *et al.* 1982; Briais *et al.*
557 1993; Wang *et al.* 2000; Hall 2002; Morley 2002; Searle 2006; Leloup *et al.* 2007; Morley 2013).
558 Based on poorly developed magnetic anomalies of presumed oceanic crust in the Central Andaman
559 Basin, seafloor spreading is widely considered to have occurred from the Pliocene (4 Ma) to Recent
560 (e.g. Kaesh Raju *et al.* 2004; Curray 2005). It follows that since 4 Ma, 118 km of spreading between
561 the Alcock and Sewell rises must have occurred at an average rate of 30 mm/yr, and must have been
562 accommodated by similar deformation along the Sagaing Fault (Kamesh Raju *et al.* 2004; Curray
563 2005). However, thick sedimentary cover within the deep axial trough of the Central Andaman Basin
564 where the youngest oceanic crust should be led Morley & Alvey (2015) to propose that oceanic
565 spreading occurred during the Late Miocene- Early Pliocene instead, and that the magnetic anomalies
566 are of insufficient quality to confirm a younger age. This means that a through-going Sagaing Fault

567 may have been developed from the Late Miocene, and that the average Pliocene-Recent slip rate of 30
568 mm/yr may be excessive.

569 In the Myanmar Central Basin positive inversion is recorded by terrestrial deposits of the Late
570 Miocene-Pliocene syn-inversion Irrawaddy Group (Bender 1983). Although the Irrawaddy Group has
571 a diachronous base and as presently understood is a poor marker for inversion onset (e.g. Sloan *et al.*
572 *this volume*), apatite fission track data support a similar Late Miocene uplift onset and a Plio-
573 Pleistocene uplift peak (Trevena *et al.* 1991). Onset of inversion in the basin has been considered to
574 be related to development of a through-going Sagaing Fault; for example by Himalayan buttressing,
575 permitted by northward motion of western Myanmar along the fault (Pivnik *et al.* 1998); or by a
576 regional kinematic reorganisation refocusing extension from the Central Basin onto the Andaman Sea,
577 as a result of Sagaing Fault connection and compounded by west-directed flow during Tibet Plateau
578 gravitational collapse (e.g. Bertrand & Rangin 2003; Rangin *et al.* 2013). Both models support
579 localisation of a through-going Sagaing Fault by the latest Miocene or start of the Pliocene (e.g.
580 Bertrand & Rangin 2003).

581 *Finite displacement and long-term slip rate*

582 Total Neogene dextral displacement across the Sagaing Fault remains poorly known, mainly due to
583 the paucity of pre-kinematic piercing points and uncertainty regarding linked tectonic structures such
584 as Andaman Sea basins (e.g. Curray 2005; Morley 2013; Morley & Alvey 2015). Upper estimates
585 including 700 km (Replumaz & Tapponnier 2003), 460 km (Curray *et al.* 1982) and 332 km (Curray
586 2005) are based on geodynamic reconstructions which assume rigid blocks and accommodation of
587 early phases of Andaman Sea oceanic spreading by the Sagaing Fault. Using a different approach,
588 Bertrand and Rangin (2003) assumed that the dextral Sagaing Fault initiated at 5 Ma, and extrapolated
589 a present-day geodetic slip rate of 20 mm/yr (Vigny *et al.* 2003) to propose a total dextral
590 displacement of 100 km. However, this estimate omits the poorly known pre-Pliocene displacement
591 reviewed above.

592 The apparent dextral offset between the Ayeyarwaddy River, where it crosses the Sagaing Fault near
593 Tagaung, and the upper Chindwin River, a proposed beheaded channel, is 425–460 km (Hla Maung
594 1987). A more conservative value using the same principle but incorporating the piercing points
595 shown in Figs. 10a and 10b is 340 km. All these values are problematic as displacement estimates
596 because the beheaded modern Chindwin River lacks the underfit valley that should be inherited from
597 a previously greater catchment (Myint Thein *et al.* 1991). It is also structurally difficult to accept such
598 large displacements near the tip of a northern strand of the Sagaing Fault which passes directly north
599 into the Chindwin basin and apparently terminates, especially when most strike-slip strain appears to
600 be focused on segments around the east of the Hukawng basin.

601 Correlation of pre-kinematic geological piercing points has proven problematic for estimating lateral
602 displacement along the Sagaing Fault. Albian limestones and serpentinites in the Tagaung-Myitkyina
603 belt, or schists and ophiolitic rocks of the Katha Gangaw belt within and to the east of the Sagaing
604 Fault northern splay, may correlate to the Mount Victoria-Kawlun belt of the Western Myanmar arc
605 system to the west, implying a post-Eocene dextral offset of >300 km (Mitchell 1977, 1981, 1993).
606 However, Myint Thein *et al.* (1991) point out that such a correlation relies on a similar geologic origin
607 and setting for the apparently offset belts, something that is yet to be proven. A lower total dextral
608 displacement estimate is based on the 203 km lateral separation of the Mayathein metamorphics – a
609 sliver of schists and gneisses on the west side of the Sagaing Fault at Tigyaing – and the remarkably
610 similar metamorphic suite exposed east of the fault at Sagaing Ridge 203 km to the south (Myint

611 Thein *et al.* 1991) (Fig. 10c). While the correlation is appealing, there are problems with this model.
612 The modern fault strand responsible for the offset likely bisects a basement sliver already uplifted by
613 transpression, so early lateral offset is excluded. It also seems unlikely that the two metamorphic areas
614 would have experienced such negligible differential vertical motion during the subsequent 203 km
615 lateral translation that they remain exposed at the same structural level.

616 Offsets of syn-tectonic piercing points have been used to calculate post-Miocene displacement and
617 slip rate along the Sagaing Fault. At Singu, syn-tectonic Pleistocene basalts possibly vented through
618 the active fault strands form a low elliptical plateau which overlies the upper part of the Plio-
619 Quaternary Irrawaddy Group and straddles the fault trace (Chhibber 1934; Bender 1983; Bertrand *et al.*
620 1998). Apparent dextral offset of the south and north margins of the plateau across the fault by 2.7
621 km and 6.5 km respectively (Fig. 11 a-c) has been considered to result from Quaternary Sagaing Fault
622 displacement (Bertrand *et al.* 1998). Five whole rock ^{40}K - ^{40}Ar ages from the basalts range from $0.25 \pm$
623 0.2 to 0.31 ± 0.02 Ma, yielding Quaternary slip rates of 10 ± 1 mm/yr to 23 ± 3 mm/yr (Bertrand *et al.*
624 1998). Although these rates are in accordance with geodetic results (discussed below), there is
625 considerable uncertainty in the position of the original margin of the plateau, and hence the amount of
626 offset. Further south, Pontian (lowermost Irrawaddy Fm.) alluvial fans containing muscovite schist,
627 ?Triassic carbonate clasts and Late Miocene Upper Pegu Group clastics at Mezaligyaung, near the
628 northern end of the Sagaing Ridge, are offset along the Sagaing Fault by about 20 km from their
629 nearest uplifted source (Myint Thein *et al.* 1991). Such a small offset could imply a very slow post-
630 Miocene slip rate of only 4 mm/yr, but it is not clear on what basis the fans have been dated, or
631 whether offset occurred immediately after deposition.

632 Aside from the very large and speculative Ayeyarwaddy/Chindwin river offset (Hla Maung 1987),
633 numerous rivers preserve variable offset where they cross the Sagaing Fault, particularly along the
634 eastern flank of Pegu Yoma (e.g. Dey 1968; Win Swe 1970; Myint Thein *et al.* 1987) where right-
635 lateral offsets of 3.7 km (Myint Thein *et al.* 1991) and 2.4 km (Wang *et al.* 2014) have been reported.
636 South of Thabeikkyin a stream is offset 1.0 km along the fault strand which re-ruptured during the
637 2012 earthquake. The stream now occupies a valley previously cut by a larger stream which has been
638 offset 1.6 km to the right and subsequently captured by headward erosion of a minor stream, lending
639 the larger stream a 0.2 km left-lateral offset where it empties into the Ayeyarwaddy River at Lower
640 Ponna. That stream now crosses an oversized delta which was formed by a much larger river, since
641 offset and captured 1.8 km to the south (Fig. 11d). Similar stream offset, up to 3 km, has been
642 reported along strike north of Thabeikkyin (Win Swe 1970).

643 There are few measurements of coseismic displacement across the Sagaing Fault. The Payagyi
644 fortress, north of Bago, was built across a strand of the fault during the 16th-century, and shows a total
645 of 5-7.5 m dextral offset of its outer wall accumulated during at least two major fault ruptures, and a
646 small contribution from the May 1930 Bago earthquake (Wang *et al.* 2011). Historical, radiometric
647 and stratigraphic constraints place construction of the fortress between 1539 and 1599, yielding a
648 range of historic slip rates from 11-18 mm/yr (Wang *et al.* 2011). Maximum coseismic dextral
649 displacement during the May 1930 earthquake is recorded south of Bago by an irrigation canal offset
650 3.2 ± 0.3 m and a stream channel offset 3.3 ± 0.2 m (Tsunami & Sato 2009). We measured a
651 maximum of 1.02 m dextral displacement of a footpath following the November 2012 M_w 6.8
652 Thabeikkyin earthquake (described below). Sixty-six years earlier, the same fault section failed during
653 the 1946 M_w 7.7 near complete rupture of the Sagaing segment (Engdahl & Villaseñor 2002; Wang *et al.*
654 2014), which originated at a latitude of $22.35 \pm 0.25^\circ\text{N}$, and may have propagated 185 km
655 northwards through Thabeikkyin and Tagaung (Hurukawa & Phyo Maung Maung 2011). Two small
656 stream offsets of 1.7-2.0 m measured south of Thabeikkyin in 2013 (described above, Fig. 4d) were

657 cut by the 2012 surface rupture, which locally contributed 0.78 m offset. The remaining ~0.9-1.2 m
658 dextral offset may be inherited 1946 coseismic displacement.

659 Assuming the 1946 event completely relaxed the segment that failed again in 2012 after a maximum
660 of 1.02 m of strain accumulation, and assuming recovery of all elastic strain during the 2012 event,
661 we calculate a 66-year average slip rate of 15.5 mm/yr, slightly lower than geodetic rates reviewed
662 below (e.g. Socquet *et al.* 2006) but consistent with the longer-term slip rates reviewed previously
663 (e.g. Bertrand *et al.* 1998; Wang *et al.* 2011). It is likely that field measurements of offset cultural
664 markers such as walls and paths significantly underestimate far-field displacement, so the calculated
665 historic slip rates should be viewed as minima.

666 *Instantaneous slip rate*

667 Models based on regional Global Positioning System (GPS) campaigns suggest that at the latitude of
668 Myanmar there is presently 35-36 mm/yr of motion between stable India and Sundaland along an
669 azimuth of 011°-014° (Socquet *et al.* 2006). Although the Sagaing Fault has been considered to be a
670 plate-bounding structure within this margin (e.g. Le Dain *et al.* 1984; Guzmàn-Speziale & Ni 1996),
671 significant off-fault strain is distributed throughout a >400 km wide shear zone straddling much of
672 Myanmar (e.g. Hla Maung 1987; Holt *et al.* 1991; Bertrand *et al.* 1998). Residual India-Sundaland
673 motion is accommodated on strike-slip structures within the Indo-Myanmar Ranges such as the
674 Thahtay Fault and Kabaw Fault, on *en echelon* folds within the Central Basin, and by highly oblique
675 slip within or elastic loading of the Andaman Trench (Le Dain *et al.* 1984; Hla Maung 1987; Pivnik *et al.*
676 1998; Nielsen *et al.* 2004; Socquet *et al.* 2006; Wang *et al.* 2014) (Fig. 12).

677 Eighteen GPS stations make up three transects across the central Sagaing Fault – one 140 km long at
678 the latitude of Mandalay, and two, each 70 km long, 35 km north and south of the main transect
679 (Vigny *et al.* 2003). The GPS transects were established in the late 1990s in addition to the four
680 regional Myanmar GPS stations of the Geodynamics of South and SE Asia project (GEODYSSSEA)
681 (Vigny *et al.* 2003). On the east (Sundaland) side of the Sagaing Fault, Ywenge station moves 6
682 mm/yr WSW relative to a stable Sundaland reference frame represented by Hpa-An station (Socquet
683 *et al.* 2006). On the western side of the fault, Kwehtaing Taung station moves 17 mm/yr to the NNW,
684 equating to a total of 18-20mm/yr of fault-parallel dextral slip across the Sagaing Fault (Vigny *et al.*
685 2003; Socquet *et al.* 2006). Similar velocities of 18 mm/yr were recorded from a GPS transect which
686 straddled several strands of the northern Sagaing Fault north of Indawgyi lake (Maurin *et al.* 2010),
687 although all statistically meaningful motion was measured across the single Kamaing segment
688 (reported as the Koma Fault).

689 Supporting GPS and historic slip rates, seismic moment tensor analysis of hypocentral data from
690 shallow earthquakes along the Sagaing Fault indicates a right-lateral slip rate of 16.4 mm/yr north of
691 Mandalay, and a rate of 11 mm/yr in the south (Radha Krishna & Sanu 2000). It should be noted that
692 these values are influenced by the rather small quantity of data for the southern area, and the statistical
693 impact of including relatively few of the largest historical earthquakes, which are widely separated in
694 time but which dominate strain release. Despite these uncertainties, generally consistent geodetic
695 results suggest that the Sagaing Fault slips rather uniformly along its length and is the most significant
696 single structure of the plate boundary, accommodating about half of India-Sundaland right-lateral
697 motion.

698 Sagaing Fault-parallel velocities from GPS stations of the Mandalay transects define an arctangent
699 curve when plotted against distance, which, with a far-field velocity of 18 mm/yr correspond to an
700 average 15 km locking depth (Vigny *et al.* 2003), also modelled as 20 km (Maurin *et al.* 2010). The

701 position of maximum modelled shear stress across the Mandalay transect is 17 km east of the Sagaing
702 Fault trace, suggesting either the unlikely scenario of a 40° easterly dip, or a significant amount of
703 dextral strain being accommodated along the Shan Scarp fault system (Vigny *et al.* 2003), for which
704 there is little evidence of neotectonic activity. Modelled locking depths of the active fault in northern
705 Myanmar range from 6-8 km, perhaps a result of a thin elastic thickness and high heat flow
706 approaching SE Tibet (Maurin *et al.* 2010) (Fig. 12).

707 **Seismicity**

708 Myanmar is characterised by extensive seismicity with a wide range of focal depths and causative
709 mechanisms (e.g. Le Dain *et al.* 1984; Guzmán-Speziale & Ni 1993; Socquet & Pubellier 2005;
710 Kundu & Gahalaut 2012; Win Swe 2012; Sloan *et al. this volume*). In the west, seismicity is
711 associated with oblique shortening across the Indo-Myanmar Ranges, thrusting within the Central
712 Basin, and an east-dipping Wadati-Benioff zone with hypocenters down to 150 km depth (e.g. Kundu
713 & Gahalaut 2012). In the east, flow around the eastern Himalayan syntaxis results in a complex
714 pattern of shallow strike-slip and extensional earthquakes (e.g. Socquet & Pubellier 2005). Against
715 this background, the Sagaing Fault is expressed by a narrow belt of shallow seismicity (<50 km),
716 dominantly strike-slip focal mechanisms, consistently steep/vertical fault-parallel nodal planes and N-
717 S trending right-lateral slip (e.g. Hurukawa & Phyo Maung Maung 2011; Kundu & Gahalaut 2012)
718 (Fig. 2c). The horizontal velocity gradient determined by GPS across the central part of the fault is
719 typical of a locked structure where deformation is accumulating elastically within the few tens of
720 kilometres either side of the active segment (Vigny *et al.* 2003). Shallow modelled locking depths
721 along the fault, as little as 6-8 km in the north, led Maurin *et al.* (2010) to suggest that some stress
722 release may be accommodated by microseismicity and aseismic creep. However, for most segments of
723 the Sagaing Fault, abundant historic records indicate that energy release by medium and large
724 earthquakes is usual.

725 *Historic seismicity*

726 Several hundred years of records document earthquake-induced damage to religious monuments built
727 along the Sagaing Fault. Such records are naturally subjective and biased towards events affecting
728 ancient cities, particularly in the Sagaing area, and neglect events along (previously) remote sections
729 of the fault in the pre-instrumental era. Collapse of pagodas in the Sagaing-Mandalay area due to
730 earthquakes is noted in the years 1429, 1469, 1485, 1588 and 1590 (Win Swe 2013). The first record
731 of a surface rupture comes from 8th June 1619 and again in 1688, on both occasions Sagaing pagodas
732 were also damaged. An earthquake in 1768 was linked to damage as far away as Bagan, while
733 earthquakes at Inn-wa in 1771, 1776 and 1830 caused local damage (Win Swe 2013). More detailed
734 observations were documented following the 1839 Amarapura earthquake (e.g. Chhibber 1934) and
735 the great 1912 Pyin-Oo-Lwin (Maymyo) earthquake, which was probably centred on the Kyaukkyan
736 Fault to the east (e.g. Coggin Brown 1917), but no detailed geological description of a Sagaing Fault
737 earthquake was made until the 2012 Thabeikkyin event (Watkinson *et al. Submitted*). Nonetheless,
738 recent work suggests that much of the Sagaing Fault has ruptured during the last 200 years, including
739 about half its length during the past 90 years (e.g. Hurukawa & Phyo Maung Maung 2011; Wang *et al.*
740 2014). Here we review historic seismicity of the last 200 years, which broadly follows a geographic
741 rupture pattern starting at the central Sagaing Fault in 1839, progressing north from 1907 to 1908,
742 before earthquake sequences in the 1930's ruptured both the northern and southern parts of the fault.
743 We conclude with observations from the most recent significant event, the 2012 Thabeikkyin
744 earthquake.

745 *Historic seismicity - central Sagaing Fault*

746 On 23rd March 1839 an earthquake apparently centred at Amarapura, 10 km south of Mandalay, killed
 747 several hundred people, damaged every brick building in Yadanapura and Ava, formed a surface
 748 rupture and caused still-visible damage to the solid brick Mingun Pagoda (Chhibber 1934; Win Swe
 749 2011, 2013) (Fig. 13a). Shaking was reported in Bhamo, Yangon and 620 km away in Mawlamyine
 750 (Win Swe 2013). It is possible that part or all of the combined 400 km long Meiktila and Sagaing
 751 segments of the Sagaing Fault ruptured (Wang *et al.* 2014) (Fig. 2c). A subsequent earthquake of M_w
 752 7.1 (Engdahl & Villaseñor 2002) caused further damage at Sagaing and Mingun on 16th July 1956
 753 (Win Swe 2013). This event, which may have re-ruptured a ~60 km long segment of the Sagaing Fault
 754 immediately south of a 1946 M_w 7.7 rupture (Engdahl & Villaseñor 2002; Hurukawa & Phyo Maung
 755 Maung 2011), was the last $M > 7.0$ earthquake along the Sagaing Fault, and the last time the fault
 756 ruptured adjacent to Sagaing and Mandalay cities. There have been no further ruptures of any part of
 757 the Meiktila segment since the speculated 1839 rupture (Wang *et al.* 2014), and the Meiktila segment
 758 now comprises much of a 260 km long seismic gap from just south of Mandalay to just south of Nay
 759 Pyi Taw (Hurukawa & Phyo Maung Maung 2011).

760 *Historic seismicity - northern Sagaing Fault*

761 Further north, an M_w 7.6 earthquake (Engdahl & Villaseñor 2002) on 27th January 1931 in Kachin
 762 State, caused damage at Karming and may have been caused by a northern strand of the Sagaing
 763 Fault, perhaps the Kamaing segment. Hurukawa and Phyo Maung Maung (2011) estimated the
 764 earthquake ruptured ~180 km of the fault. Earlier earthquakes of M_w 7.0 in 1906 and M_w 7.5 in 1908
 765 in the same area support a stick-slip mechanism for the northern Sagaing Fault (Maurin *et al.* 2010). A
 766 further $M 7.0$ event on 18th August 1950 is reported by Win Swe (2013) in the same area, but is
 767 reviewed neither by Engdahl and Villaseñor (2002) nor by Hurukawa and Phyo Maung Maung (2011).
 768 The 1946 Wuntho earthquake sequence culminated in a M_w 7.7 earthquake (Engdahl & Villaseñor
 769 2002) on 12th September, which may have ruptured a 185 km long segment of the Sagaing Fault
 770 through Tagaung and Thabeikkyin (Hurukawa & Phyo Maung Maung 2011). Remarkably the 1946
 771 M_w 7.7 event occurred three minutes after a M_w 7.3 earthquake (Engdahl & Villaseñor 2002) which
 772 ruptured at least 80 km of the Indaw segment to the north (Wang *et al.* 2014), and possibly up to 155
 773 km, towards the southern tip of the 1931 Kachin rupture (Hurukawa & Phyo Maung Maung 2011).

774 A 5th January 1991 M_w 7.0 earthquake (Engdahl & Villaseñor 2002) north of Tagaung caused damage
 775 as far south as Thabeikkyin, and may have re-ruptured 49 km of the 1946 slip segments, up to the
 776 location of a June 1992 $M 6.3$ aftershock near Indaw (Win Swe 2011; Hurukawa & Phyo Maung
 777 Maung 2011).

778 *Historic seismicity - southern Sagaing Fault*

779 Historical documentation of southern Sagaing Fault earthquakes includes records of damage to
 780 Shwemawdaw Pagoda at Bago (built 307 BC), which was damaged by earthquakes 33 times in the
 781 2114 years from 197 BC to 1917 AD (Win Swe, 2011), on average once every 64 years. In 1930 the
 782 pagoda collapsed once again and 500 people were killed when the southern end of the Sagaing Fault
 783 failed in the first of two closely spaced earthquakes of M_w 7.2 and M_w 7.3 (Engdahl & Villaseñor
 784 2002) about 120 km apart at Bago (5th May 1930) and Pyu (3rd December 1930) (Chhibber 1934).
 785 Their proximity in space and time indicates that Coulomb stress changes resulting from the Bago
 786 event may have triggered the Pyu event (Tsutsumi & Sato 2009), in a sequence remarkably similar to
 787 the North Anatolian Fault's M_w 7.4 and M_w 7.1 Izmit and Düzce earthquakes of August and November
 788 1999 (e.g. Utkucu *et al.* 2003). The Bago event ruptured between 100 km (Wang *et al.* 2011) and 131

789 km of the Sagaing Fault (Hurukawa & Phyo Maung Maung 2011) and caused ≥ 3 m of coseismic
790 dextral surface displacement, yielding a recurrence interval of ≥ 160 years (Tsutsumi & Sato 2009).
791 The 16th-century Payagyi fortress lies near the northern end of the Bago rupture, and displays 6 m of
792 dextral displacement (Wang *et al.* 2011). This displacement was accumulated mainly during two
793 strong earthquakes since construction and may have been further slightly offset by the 1930 Bago
794 earthquake, yielding a recurrence interval of one to two centuries, assuming a uniform slip model
795 (Wang *et al.* 2011). The subsequent Pyu event in December 1930 propagated northward from the
796 proposed northern termination of the Bago rupture, and ruptured a further 120 km of the Sagaing
797 Fault (Hurukawa & Phyo Maung Maung 2011) (Fig. 2c).

798 An earlier $M \sim 7.0$ earthquake on August 8th 1929 bent railway lines at Swa, near Taungoo (Le Dain *et al.*
799 *al.* 1984; Win Swe 2011). Located at the northern end of the proposed 1930 Pyu rupture on the eastern
800 'shortcut' strand of the Nay Pyi Taw segment, the 1929 event could have contributed to triggering the
801 1930 earthquake series.

802 *2012 Thabeikkyin earthquake*

803 The most recent significant earthquake generated by the Sagaing Fault was the 11th November 2012
804 M_w 6.8 Thabeikkyin earthquake, which ruptured a ~ 45 km long part of the Sagaing segment between
805 Singu and Sabeanago (Fig. 2c). Centroid moment tensor solutions of the primary event and seven
806 largest aftershocks indicate dextral slip along north-south trending, steeply east dipping to sub-vertical
807 strands of the Sagaing Fault. Aftershocks continued for several months, including clusters of small
808 earthquakes at the northern end of the Sagaing Fault and close to Nay Pyi Taw in the south. Twenty
809 six people were killed and 231 were injured by the mainshock, which occurred at 06.30 local time on
810 a Sunday. Many buildings, including 201 houses, 25 schools, 13 health centres and 35 monasteries
811 were destroyed or severely damaged (Fig. 13b); clearly the fortuitous timing of the earthquake meant
812 many public buildings were unoccupied, significantly reducing casualty numbers (Ko Ko Gyi *et al.*
813 2012). Damage was most severe in towns lining the Ayeyarwaddy River, particularly those on the east
814 bank including Sabeanago, Thabeikkyin, and Kule. Much of the most severe damage was due to
815 gravitational slumping down river banks, particularly in towns beyond the rupture tips such as Male.

816 A well developed 45 km long surface rupture was associated with the 2012 Thabeikkyin earthquake,
817 trending almost exactly N-S (001°) on or close to the line of longitude 95.975° E. For much of its
818 length the surface rupture broadly followed the Ayeyarwaddy River, lying in a valley on the east bank,
819 separated from the river by narrow pressure ridges. The surface rupture was expressed by *en echelon*
820 sigmoidal Riedel shears (Fig. 13c) arranged into small arrays reflecting shallow upwards splaying and
821 curvature of the rupture, and larger arrays that may mimic the segmented geometry of the seismogenic
822 Sagaing Fault at depth. Maximum dextral strike-slip displacement of 1.02 m, recorded north of
823 Thabeikkyin, was accommodated across the shears themselves, across the inter-shear linkages, and
824 across a zone of horizontal flexure at least 5 m wide either side of the surface rupture. A number of
825 small releasing step-overs along the length of the surface rupture were associated with existing or
826 incipient sag ponds, locally associated with up to 1.17 m of coseismic subsidence. Liquefaction along
827 the surface rupture resulted in injection of mud and sand into dilation fractures and localised mud
828 volcanoes, notably near Singu.

829 The surface rupture terminated in the south within and around Kyet Phyu Taung lake, 4 km north of
830 Singu. The lake is part of a broad depression close to where the Ayeyarwaddy River resumes its
831 course along the Sagaing Fault and becomes braided after flowing in a narrow confined channel
832 around the Singu basalt plateau. Multiple sets of mole tracks and transpressional splaying structures

833 associated with 0.5 m of uplift and widely distributed strike-slip indicate that the rupture terminated in
834 a complex horsetail splay, perhaps as it attempted to cross the 1.5 km wide releasing step-over marked
835 by Kyet Phyu Taung lake. In the north the rupture terminated in a smaller array 160 m wide near
836 Kyauk Myae village on the west river bank.

837 Discussion

838 *Tectonic evolution*

839 The development of the Sagaing Fault can be summarised broadly as northwards-younging
840 localisation of discrete strike-slip fault segments from a long-lived zone of diffuse dextral shear along
841 the eastern margin of India (Fig. 14). Early dextral transpression along this margin (Fig. 14a) has been
842 driven by the northward motion and indentation of Greater India into Eurasia during the Himalayan
843 Orogeny since the Early Eocene and perhaps earlier, though the size of Greater India, the timing of
844 the continent's passage past Myanmar and the extent of strike-slip partitioning within Sundaland
845 remain unclear (e.g. Tapponnier *et al.* 1982; Treolar & Coward 1991; Replumaz & Tapponnier 2003;
846 Aitchison *et al.* 2007; van Hinsbergen *et al.* 2011; Hall 2012; Morley 2013). Emplacement of the
847 Naga Hills ophiolite, part of the Western Ophiolite Belt, represents this phase of oblique contraction
848 and occurred by the Mid-Eocene, somewhat later than Early Cretaceous emplacement of the Mt.
849 Victoria and Chin Hills ophiolites (Acharyya 2007). During the Eo-Oligocene the Mogok
850 Metamorphic Belt, lying at the core of a belt of dextral shear, experienced peak high temperature
851 metamorphism, while the Mae Ping and Three Pagodas faults of NW Thailand experienced the final
852 phases of sinistral shear (e.g. Lacassin *et al.* 1997; Searle *et al.* 2007; Morley *et al.* 2011) (Fig. 14a).

853 The Late Oligocene to Early Miocene coupling of western Myanmar and India (e.g. Curray 2005;
854 Searle & Morley 2011) led to a more direct requirement for dextral shear within central Myanmar,
855 whose earliest expression may be a diffuse zone of dextral slip initiated during the late Paleogene
856 (Fig. 14b), which generated deep-seated structural fabrics subsequently reactivated as strands of the
857 Neogene strike-slip fault system (e.g. Le Dain *et al.* 1984; Bertrand & Rangin 2003; Socquet &
858 Pubellier 2005). Long-lived faults of the Shan Plateau, such as the Kyaukkyan/Mae Ping, Panlaung
859 and Taungoo faults, may have played a part in this early shear zone.

860 Development of a more discrete region of strike-slip may have its origins in a zone of dextral
861 transtension west of the Mergui-North Sumatra Basin, at the southernmost end of the Sagaing Fault at
862 about 32 Ma (Polachan & Racey 1994; Curray 2005). The 'South Sagaing Fault' segment, which
863 bounds a Late Oligocene-Early Miocene basin, could represent the site of earliest localised dextral
864 motion (Morley 2013) (Fig. 14b).

865 Ductile stretching and diachronous cooling within the Shan Scarp and Mogok Metamorphic Belt in
866 Myanmar and the Gaoligong Shan and Chongshan in Yunnan from Late Eocene to Mid-Miocene
867 times (Wang & Burchfiel 1997; Bertrand *et al.* 2001; Bertrand & Rangin 2003; Socquet & Pubellier
868 2005; Akciz *et al.* 2008; Zhang *et al.* 2012) support a wave of northward migrating dextral shear that
869 shortly pre-dated localisation of strain along more northerly segments of the Sagaing Fault (Socquet
870 & Pubellier 2005) (Fig. 14c, d). Cessation of Late Oligocene to Early Miocene dextral strike-slip
871 basin development in northern Thailand (Morley 2004; Morley *et al.* 2011) may indicate eastwards
872 transferral of dextral slip from the Shan Plateau (resulting in stress relaxation and Early-Mid-Miocene
873 metamorphic core complex exhumation in northern Thailand) and onto central parts of the Sagaing
874 Fault or possible precursor strands along the Shan Scarp fault zone (Searle & Morley 2011; Morley &
875 Alvey 2015) (Fig. 14e). The youngest cooling ages from the exhumed metamorphic belts represent

876 final cessation of transtensional ductile stretching, and also correspond to the Mid/Late Miocene (11
877 Ma) onset of localised inversion in the Central Basin (e.g. Wang & Burchfiel 1997; Pivnik *et al.* 1998;
878 Bertrand & Rangin 2003; Akciz *et al.* 2008; Zhang *et al.* 2012) (Fig. 14f).

879 At the same time Mid-Miocene high-K calc-alkaline volcanic rocks of Mount Popa in central
880 Myanmar provide the final definitive record of eastward subduction-related magmatism beneath
881 Myanmar (Lee *et al.* 2010), which likely started in the Early Oligocene (Mitchell 1993). Pleistocene
882 high-Al basalts and absarokites at Mount Popa and Monywa and OIB-type alkali basalts at Singu
883 (Bertrand *et al.* 1998; Lee *et al.* 2010) have been previously attributed to continued post-Miocene
884 subduction (e.g. Mitchell 1993), but more recent work suggests they formed by extension-related
885 melting of subduction-enriched mantle, indicating possible Mid-Miocene (11 Ma) cessation of
886 subduction (Everett *et al.* 1990; Lee *et al.* 2010). However, the timing of subduction and possible
887 modern continuation remains contentious. An east-dipping slab below the Indo-Myanmar Ranges is
888 revealed by mantle topography and earthquake data (e.g. Mukhopadhyay & Dasgupta 1988; Li *et al.*
889 2008), and there is evidence of historic megathrust earthquakes along the western Myanmar coast
890 (Wang *et al.* 2011). Despite this, earthquakes within the east-dipping Benioff zone are dominantly
891 intra-slab strike-slip events and not interface thrusts, indicating that the slab is not presently being
892 subducted but is being translated northwards (Kundu & Gahalaut 2012). Mid-Miocene cessation of
893 subduction would have placed greater emphasis on the Sagaing Fault to accommodate lateral motion
894 between India/western Myanmar and Sundaland, and a more fully localised fault system was
895 developed (e.g. Socquet & Pubellier 2005).

896 Late Miocene to Pliocene (Morley & Alvey 2015) or Early Pliocene to Recent (Curry 2005) oceanic
897 spreading of 118 km in the Andaman Sea between the Alcock and Sewell rises was likely directly
898 connected to the Sagaing Fault and resulted in the same amount of dextral slip along a fully localised
899 structure (Kamesh Raju *et al.* 2004; Curry 2005) (Fig. 14g). An Early Pliocene to Recent period of
900 sea floor spreading directly connected to the Sagaing Fault results in a strike-slip rate of ~30 mm/yr,
901 significantly higher than post-Pliocene rates and modern geodetic rates. However, a thick sedimentary
902 package burying the spreading centre suggests that spreading occurred earlier (Morley & Alvey
903 2015), allowing more time for accumulation of 118 km of displacement at a rate more consistent with
904 observations. Assuming sea floor spreading was complete by Early Pliocene times, an additional ~70
905 km of strike-slip displacement may have been accumulated at an assumed average rate of ~18 mm/yr.
906 This displacement could have been accommodated by episodic extension and late sea floor spreading
907 in the Andaman Sea (Morley & Alvey 2015).

908 At the same time Late Miocene to Pliocene onset of widespread positive inversion in the Central
909 Basin is recorded by the poorly dated syn-inversion Irrawaddy Group and apatite fission track ages
910 (Trevena *et al.* 1991; Pivnik *et al.* 1998; Sloan *et al. this volume*). Extreme thinning/sea-floor
911 spreading in the Andaman Sea and inversion in the Central Basin may be related to a regional-scale
912 kinematic reorganisation that was facilitated by localisation of the Sagaing Fault by the start of the
913 Pliocene at the latest, and probably during the Late Miocene (e.g. Bertrand & Rangin 2003). By this
914 time more than half of the total dextral shear across Myanmar may have already been accumulated
915 across a distributed array of precursor fault systems and shear zones by a rather different process
916 perhaps more similar to continuum mechanics (e.g. England & Molnar 2005).

917 Northernmost strands of the Sagaing Fault curve to the NW into structures such as the Lohit and Main
918 Central thrusts. Parts of the termination array have been rotated into a releasing geometry by crustal
919 flow from the Tibetan Plateau around the eastern Himalayan syntaxis (Rangin *et al.* 2013). Extension
920 across the rotated northern termination splays may not be of the same magnitude as extension in the

921 Andaman Sea, but geomorphic similarities with global examples of extreme continental extension
 922 resulting in ‘basin and range’-style topography (e.g. Coney & Harms 1984; Armijo *et al.* 1986;
 923 Rhodes *et al.* 2005; Genç & Yürür 2010) suggest significant extension has occurred immediately
 924 south of the eastern Himalayan syntaxis. Shallow normal fault focal mechanisms from the NEIC
 925 catalogue within and around the margins of the Bhamo Basin support modern extension. In many
 926 regions of basin and range extension, mid-lower crustal rocks are exposed below low-angle normal
 927 faults in metamorphic core complexes (e.g. Coney & Harms 1984; Macdonald *et al.* 1993; Whitney *et al.*
 928 *al.* 2013). It has been suggested that rocks of the Mogok Metamorphic Belt may be genetically linked
 929 with metamorphic core complexes in northern Thailand (Searle *et al.* 2007), although the timing and
 930 direction of unroofing of these two areas is not the same (Searle & Morley 2011). Nonetheless,
 931 exhumation of other poorly known ranges of metamorphic rocks associated with the northern Sagaing
 932 Fault, such as the Katha-Gangaw belt (Mitchell *et al.* 2007; Searle *et al.* 2007), should not be assumed
 933 to be the result of transpression, a strike-slip driven extensional metamorphic core complex
 934 mechanism must also be considered.

935 *Present day structural continuity and seismic potential*

936 Major faults form from the linkage and coalescence of smaller segments, removal of complexities
 937 such as bends, step-overs, splays and rotation of pre-existing fabrics into parallelism with the through-
 938 going fault. These processes are promoted at high shear strains (e.g. Spyropoulos *et al.* 1999). The
 939 North Anatolian Fault (total slip: ~35 km), for example, is presently more segmented than the San
 940 Andreas Fault (total slip: ~250 km) (Scholz 2002). Empirical results suggest that maximum
 941 earthquake potential is proportional to the length of ruptured segments (e.g. Wells & Coppersmith
 942 1994), so that faults become capable of generating larger magnitude earthquakes as their cumulative
 943 displacement and hence segment length increases.

944 Additionally, like the San Andreas Fault, the Chaman Fault (the Sagaing Fault’s sinistral counterpart
 945 bounding the western margin of India) and the Sumatran Fault south of the Andaman Sea, the Sagaing
 946 Fault is considered to be so continuous that its central 700 km has been classed as an ‘earthquake fault
 947 superhighway’, capable of supershear ruptures (Robinson *et al.* 2010). Supershear occurs when
 948 rupture speed exceeds S-wave or even P-wave speed, resulting in Mach shock cones and increased
 949 ground acceleration, and is more likely on long continuous faults along which rupture can accelerate
 950 without interruption from fault heterogeneities (e.g. Kostrov & Das 1988; Bernard & Baumont 2005;
 951 Robinson *et al.* 2010). Consequently, important questions about the modern Sagaing Fault are: 1)
 952 whether it is as continuous as its gross geomorphology suggests (e.g. Le Dain *et al.* 1984; Vigny *et al.*
 953 2003); 2) whether it possesses step-overs between its segments (e.g. Wang *et al.* 2014); and 3)
 954 whether these are large enough to arrest or slow down seismic ruptures (e.g. Wesnousky 2006;
 955 Robinson *et al.* 2010).

956 Prominent releasing step-overs and bends, such as are occupied by lakes Indaw and Indawgyi (Figs.
 957 8b & c), characterise the northern splays of the Sagaing Fault. Indaw Lake, a step-over ≤ 2.5 km wide,
 958 has a similar size, geometry and structural setting as Lake Sapanca, Turkey, which separates the
 959 Sapanca and Sakarya segments of the North Anatolian Fault. Despite its 1-2 km step-over width, the
 960 Sapanca step-over failed to arrest the 17th August 1999 M_w 7.4 Izmit earthquake (Lettis *et al.* 2002),
 961 in the same way that the Indaw step-over was likely breached by the first (M_w 7.3) of the Sagaing
 962 Fault’s twin 1946 earthquakes which probably ruptured the Indaw and Mawlu segments (Hurukawa &
 963 Phyo Maung Maung 2011; Wang *et al.* 2014). Indawgyi is significantly wider than Indaw and Lake
 964 Sapanca, but may be bypassed by a through-going fault below alluvial fans on its southern side.

965 Several step-overs were revealed along the 2012 Thabeikkyin surface rupture of the apparently
966 continuous central part of the Sagaing segment, including south of Thabeikkyin city (Fig. 8d), and at
967 Lower Ponna (Fig. 11d). Each of these was clearly breached by the fault rupture, and it is likely that
968 they reflect either upward curvature of fractures within unconsolidated overburden from a simple and
969 continuous basement fault, or minor/shallow segmentation of the basement fault only (Fig. 15a).
970 Helicoidal upward curvature of shears forming *en echelon* surface patterns is well known from
971 analogue models (e.g. Mandl 1988; Richard *et al.* 1995) and similarities between models and natural
972 examples have been recognised (e.g. Dooley & McClay 1997). This process may mask fault
973 simplicity at the depth of large earthquake nucleation (Graymer *et al.* 2007) or even immediately
974 below the surface sediment layer, as was observed in the 2001 Kunlun earthquake (e.g. Lin &
975 Nishikawa 2011). Such a process may also be responsible for Sagaing Fault step-overs such as Yega
976 In (Fig. 9b) and those along the Meiktila segment (Fig. 4b) as well as smaller-scale shallow
977 complexities (Fig. 15b). Nonetheless, the 2012 rupture terminated at the 1.5 km wide Kyet Phyu
978 Taung lake step-over, indicating that the lake marks genuine basement fault segmentation.

979 The Nay Pyi Taw double bend is the most significant complexity along the superficially most
980 continuous central 700 km of the Sagaing Fault. Though it comprises a 10 km wide releasing bend
981 and a segmented restraining bend (Fig. 9c), the entire system is bypassed by an apparently continuous
982 shortcut fault (Wang *et al.* 2014) that would be preferentially exploited by a high speed rupture.
983 Similarly, the prominent restraining bend between the Bago and Pyu segments (Fig. 9d) is breached at
984 the surface by almost continuous reverse faults, and is less than 1 km wide in any case.

985 Even if supershear rupture is limited by the fault heterogeneities discussed above, coseismic strain
986 transfer across step-overs can still be accommodated by stress transfer or hard linkage (Scholz 2002).
987 The efficacy of such transfer is a function of the source magnitude/displacement characteristics and
988 the width of the step-over (e.g. Lettis *et al.* 2002; Wesnousky 2006). Step-overs 1-2 km wide are
989 found to be breached by most historic earthquakes (Lettis *et al.* 2002), while those 3-4 km
990 (Wesnousky 2006) or 4-5 km wide (Lettis *et al.* 2002) arrest most historic earthquakes. It is clear that
991 the onshore Sagaing Fault possesses no step-overs wider than about 2.5 km, with the possible
992 exception of the poorly exposed region between the Sagaing and Meiktila segments (Wang *et al.*
993 2014), which may mark a releasing structure 4 km wide. Sagaing Fault earthquakes possibly arrested
994 by step-overs include the 1930 Pyu (18°N restraining bend), 1946 Wuntho (southern Indaw segment
995 step-over), 1956 Sagaing (Southern Sagaing segment step-over) (Wang *et al.* 2014), and the 2012
996 Thabeikkyin (Kyet Phyu Maung lake step-over) earthquakes.

997 Segment boundaries aside, all five of the main segments south of the northern splay possess
998 apparently uninterrupted portions >100 km long. Though not as great as the 700 km continuous
999 supershear segment originally proposed, it remains possible that that the Sagaing Fault is an
1000 'earthquake fault superhighway' as defined by Robinson *et al.* (2010). Critical unanswered questions
1001 include: can identified structural complexity, though not significant enough to terminate a rupture,
1002 reduce rupture velocity below supershear speeds?; and is structural complexity at the surface a
1003 reliable expression of fault geometry at seismogenic depths?

1004 When considering the seismic hazard of the Sagaing Fault, there clearly remain significant
1005 uncertainties about the fault's seismic cycle, segmentation, off-fault strain distribution and the
1006 contribution of aseismic creep. Wang *et al.* (2014) proposed maximum magnitudes for full single
1007 segment rupture earthquakes along the Bago, Pyu, Nay Pyi Taw, Meiktila and Sagaing segments as
1008 7.7, 7.5, 7.1-7.2, 7.8-7.9, 7.7 respectively, and for the northern segments from 7.0-7.2 (Tawma
1009 segment) to 7.9-8.0 (Mogang segment). These estimates are supported by the series of M>7.0
1010 earthquakes that ruptured over half of the entire fault during the first half of the twentieth century (e.g.

1011 Hurukawa & Phyo Maung Maung 2011; Wang *et al.* 2014). Based on analysis of historical seismicity
 1012 and tectonic geomorphology Wang *et al.* (2014) additionally suggest whole segment failures resulting
 1013 in $\sim M_w$ 7.7 earthquakes should occur every 300-400 years, and that partial segment failures expressed
 1014 by M_w 6.8 to M_w 7.0 earthquakes have short decadal recurrence intervals. Examples of the latter
 1015 include the partial failure of the Sagaing segment at Thabeikkyin in 2012 just 66 years after the 1946
 1016 M_w 7.7 failure, and the failure of the Indaw segment in both 1946 and 1991. Recurrence of 1930-type
 1017 events along the Bago segment is likely to be >160 years (Tsutsumi & Sato 2009), but recurrence of
 1018 any earthquake close to Bago (i.e. including both the Pyu and Bago segments) is likely to be between
 1019 90 and 115 years (Wang *et al.* 2011).

1020 Two long sections of the Sagaing Fault lack clear records of historic seismicity (Hurukawa & Phyo
 1021 Maung Maung 2011). A ~ 180 km long section in the Andaman Sea south of 16.6°N lacks historic
 1022 seismicity since at least 1897, and a ~ 260 km long section straddling the Nay Pyi Taw and Meiktila
 1023 segments similarly lacks seismicity, with the last probable rupture of the Meiktila segment being the
 1024 1839 Amarapura event (Tsutsumi & Sato 2009; Wang *et al.* 2014). Complete failure of these segments
 1025 would result in $>M7.7$ and $M7.9$ earthquakes respectively according to empirical magnitude-length
 1026 relationships (Tsutsumi & Sato 2009). Assuming a conservative 18 mm/yr instantaneous slip rate (e.g.
 1027 Maurin *et al.* 2010) for the whole Sagaing Fault, ~ 3.2 m of displacement has accumulated across the
 1028 Nay Pyi Taw seismic gap between 1839 and 2015. Citing evidence that the 1839 rupture breached the
 1029 Meiktila-Sagaing segment boundary, Wang *et al.* (2014) go further to propose a scenario whereby
 1030 both segments fail together, resulting in a M_w 8.1-8.3 event with a recurrence interval of 500-1000
 1031 years. However, it is not yet known what contribution, if any, there is from aseismic creep along
 1032 segments well-constrained by GPS surveys (e.g. Maurin *et al.* 2010), much less the understudied
 1033 Meiktila and Nay Pyi Taw segments.

1034 **Concluding remarks**

1035 The localised and continuous modern Sagaing Fault can be considered as a relatively young (Late to
 1036 post-Miocene) structure that accommodated about 100-118 km of localised dextral strike-slip strain
 1037 since the onset of Andaman Sea spreading (e.g. Bertrand & Rangin 2003; Kamesh Raju *et al.* 2004;
 1038 Curray 2005; Morley & Alvey 2015), despite its position on a more diffuse and longer-lived dextral
 1039 boundary zone perhaps >200 km wide. This zone may have accommodated a total of 300-700 km
 1040 offset since the Eo-Oligocene, along structures including the Shan Plateau metamorphic belts and
 1041 associated upper crustal fault systems now largely eroded, the Shan Scarp/Kyaukkyan fault systems,
 1042 the faults of western Thailand as well as embryonic strands of the Sagaing Fault (e.g. Mitchell 1977,
 1043 1981, 1993; Curray *et al.* 1982; Replumaz & Tapponnier 2003; Curray 2005; Morley 2013). This
 1044 represents the transition from Pre-Pliocene continuum mechanics, whereby the Myanmar crust above
 1045 eastward subduction was deforming as a thin sheet with spaced strike-slip faults of relatively small
 1046 local displacement, such as is currently happening in much of central Asia (e.g. England & Molnar
 1047 2005); to a Pliocene-Recent high strain zone of nearly continuous localised faulting from the
 1048 Andaman Sea towards the eastern Himalayan syntaxis. Localisation at the fault's current position,
 1049 rather than along longer-lived structures such as the Kyaukkyan/Mae Ping fault system or Shan Scarp
 1050 Fault is probably a result of northward propagation of fault systems at the northern end of the
 1051 Andaman Sea (e.g. Morley 2013), coupled with thermally weakened lithosphere at the margin of the
 1052 Myanmar Central Basin.

1053 The Sagaing Fault's structural continuity, high slip rate and tendency to produce large (possibly
 1054 supershear) earthquakes means it has a high seismic hazard and poses a great risk to the cities that lie
 1055 along or close to it, particularly Yangon, Bago, Nay Pyi Taw, Mandalay and Myitkyina (Robinson *et*

1056 *al.* 2010; Yeats 2012). Historical earthquakes in Myanmar have had relatively small death tolls, the
 1057 worst on record being the 1930 Bago earthquake, which killed 550 people (e.g. Win Swe 2011).
 1058 However, in contrast to 1930, Myanmar's population is now 51.5 million, an increase of 350% since
 1059 the 1931 census (Department of Population, Ministry of Immigration and Population 2015). Twenty
 1060 million people alone currently live in the nineteen districts cut by the Sagaing Fault, of whom almost
 1061 half live in urban settings (Department of Population, Ministry of Immigration and Population 2015),
 1062 many within a few kilometres of the Sagaing Fault and often close to major rivers, both factors that
 1063 dramatically increase the likelihood of earthquake damage (Luo *et al.* 2012). In Mandalay urban
 1064 population has increased from 163,527 (1948) to its present level of 1,225,546 (Andrus 1948;
 1065 Department of Population, Ministry of Immigration and Population 2015), indicating a
 1066 disproportionate urban growth rate likely observed in numerous cities along the fault. Urban
 1067 population growth and increased building fragility led Wyss (2005) to propose a 3-60 times increase
 1068 in expected casualties for repeat earthquakes in India compared to measured losses in the last century,
 1069 a calculation that could be applied to the next Bago or Amarapura (Mandalay) earthquake, for
 1070 example.

1071 An additional factor which increases the risk resulting from Sagaing Fault seismic hazard is
 1072 corruption in the public sector. Anomalously high earthquake death tolls are associated with corrupt
 1073 countries; devastating earthquakes in Haiti (2010) and Pakistan (2005), for example, were made worse
 1074 by corruption in construction industries (Ambraseys & Bilham 2011). In 2014 Myanmar was ranked
 1075 amongst the 20 most corrupt countries in the world, alongside Haiti and worse than Pakistan
 1076 (Transparency International 2014). To mitigate the risk posed by the Sagaing Fault it is essential that
 1077 work to improve transparency in the building industry, overall building quality and public awareness
 1078 along the fault is carried out alongside future structural, geodetic and palaeoseismic studies.

1079 **Acknowledgements**

1080 We would like to thank Lin Thu Aung, Myo Thant, Thura Aung, the Myanmar Earthquake Committee
 1081 and the Department for Hydrology and Meteorology for their assistance during fieldwork. We are
 1082 grateful for valuable discussions with Hla Hla Aung, Kerry Sieh, Wang Yu and Soe Min during
 1083 preparation of this manuscript. We would also like to thank Chris Morley and an anonymous reviewer
 1084 for their constructive reviews that improved the final manuscript. Fieldwork along the Sagaing Fault
 1085 was partly funded by NERC Urgency Grant NE/K016474/1.

1086 **References**

- 1087 ACHARYYA, S. K. 2007. Collisional emplacement history of the Naga-Andaman ophiolites and the
 1088 position of the eastern Indian suture. *Journal of Asian Earth Sciences*, **29**, 229-242.
 1089 AITCHISON, J. C., ALI, J. R. & DAVIS, A. M. 2007. When and where did India and Asia collide?.
 1090 *Journal of Geophysical Research*, **112**, B05423, doi:10.1029/2006JB004706.
 1091 AKCIZ, S., BURCHFIEL, B. C., CROWLEY, J. L., YIN, J. Y. & CHEN, L. Z. 2008. Geometry, kinematics,
 1092 and regional significance of the Chong Shan shear zone, Eastern Himalayan Syntaxis,
 1093 Yunnan, China. *Geosphere*, **4**, 292-314.
 1094 AMBRASEYS, N. & BILHAM, R. 2011. Corruption Kills. *Nature*, **469**, 153-155.
 1095 ANDRUS, J. R. 1948. Burmese Economic Life. Stanford University Press, Stanford, California. 362 pp.
 1096 ARMIJO, R., TAPPONNIER, P., MERCIER, J. L. & HAN TONG-LIN. 1986. Quaternary extension in
 1097 southern Tibet: field observations and tectonic implications. *Journal of Geophysical*
 1098 *Research*, **91**, 13,803–13,872.

- 1099 ARMIJO, A., MEYER, B., HUBERT, A. & BARKA, A. 1999. Westward propagation of the North
1100 Anatolian fault into the northern Aegean: Timing and kinematics. *Geology*, **27**, 267-270.
- 1101 AUNG KHIN, AUNG TIN U, AUNG SOE & KHIN HAN. 1970. A study on the gravity indication of the
1102 Shan Scarp fault. *Union of Burma Journal of Science and Technology*, **3**, 91-113.
- 1103 BARBER, A. J. & CROW, M. J. 2009. Structure of Sumatra and its implications for the tectonic
1104 assembly of Southeast Asia and the destruction of Paleotethys. *Island Arc*, **18**, 3-20.
- 1105 BARLEY, M. E., PICKARD, A. L. KHIN ZAW, RAK, P. & DOYLE, M. G. 2003. Jurassic to Miocene
1106 magmatism and metamorphism in the Mogok metamorphic belt and the India-Eurasia
1107 collision in Myanmar. *Tectonics*, **22**, doi: 10.1029/2002TC001398.
- 1108 BENDER, F. 1983. Geology of Burma. In: BENDER, F., JACOBSHAGEN, V., DE JONG, J. D., & LUTIG, G.,
1109 (eds.), *The Regional Geology of the Earth Series*, **16**. Berlin, Germany, 293 pp.
- 1110 BERNARD, P. & BAUMONT, D. 2005. Shear Mach wave characterization for kinematic fault rupture
1111 models with constant supershear rupture velocity. *Geophysical Journal International*, **162**,
1112 431-447.
- 1113 BERTRAND, G. & RANGIN, C. 2003. Tectonics of the western margin of the Shan plateau (central
1114 Myanmar): implication for the India-Indochina oblique convergence since the Oligocene.
1115 *Journal of Asian Earth Sciences*, **21**, 1139-1157.
- 1116 BERTRAND, G., RANGIN, C., MAURY, R. C., HLA MYO HTUN, BELLON, H. & GUILLAUD, J-P. 1998. Les
1117 basalts de Singu (Myanmar): nouvelles contraintes sur le taux de décrochement recent de la
1118 faille de Sagaing. *Earth and Planetary Sciences*, **327**, 479-484.
- 1119 BERTRAND, G., RANGIN, C., MALUSKI, H., HAN, T. A. THEIN, M., MYINT, O. MAW, W. & LWIN, S.
1120 1999. Cenozoic metamorphism along the Shan scarp (Myanmar): evidences for ductile shear
1121 along the Sagaing fault or the northward migration of the eastern Himalayan syntaxis?
1122 *Geophysical Research Letters*, **26**, 915-8.
- 1123 BERTRAND, G., RANGIN, C., MALUSKI, H., BELLON, H. & THE GIAC SCIENTIFIC PARTY. 2001.
1124 Diachronous cooling along the Mogok Metamorphic Belt (Shan Scarp, Myanmar): the trace
1125 of the northward migration of the Indian syntaxis. *Journal of Asian Earth Sciences*, **19**, 649-
1126 659.
- 1127 BRIAIS, A., PATRIAT, P. & TAPPONNIER, P. 1993. Updated interpretation of magnetic anomalies and
1128 seafloor spreading stages in the South China Sea: Implications for the Tertiary tectonics of
1129 Southeast Asia. *Journal of Geophysical Research*, **98**, 6299-6328.
- 1130 BUNOPAS, S. 1981. Palaeogeographic history of western Thailand and adjacent parts of southeast Asia
1131 – a plate-tectonic interpretation. Ph.D. Thesis. University of Wellington, New Zealand –
1132 reprinted as Geological Survey Paper No. 5, Department of Mineral Resources, Bangkok,
1133 Thailand, 810 pp.
- 1134 CHAMOT-ROOKE, N., RANGIN, C. & NIELSEN, C. 2001. Timing and kinematics of Andaman basin
1135 opening. *Eos Transactions Supplement*, 82 (20).
- 1136 CHÂRUSIRI, P., CLARK, A. H., FARRAR, E., ARCHIBALD, D. & CHÂRUSIRI, B. 1993. Granite belts in
1137 Thailand: evidence from the ⁴⁰Ar/³⁹Ar geochronological and geological syntheses. *Journal*
1138 *of Southeast Asian Earth Sciences*, **8**, 127-136.
- 1139 CHHIBBER, H. L. 1934. The Geology of Burma. Macmillan and Co., London, 538 pp.
- 1140 CHRISTIE-BLICK, N. & BIDDLE, K. T. 1985. Deformation and basin formation along strike-slip faults.
1141 In: BIDDLE, K. T., & CHRISTIE-BLICK, N. (eds), *Strike-slip deformation, basin formation and*
1142 *sedimentation*. *Society of Economic Paleontologists and Mineralogists*, Special Publication,
1143 **37**, 1-34.
- 1144 COGGIN BROWN, J. 1917. The Burma earthquake of May 1912. *Memoirs of the Geological Survey of*
1145 *India*, **42**, 1-147.
- 1146 COGGIN BROWN, J. & LEICESTER, P. 1933. The Pyu earthquake of 3rd and 4th December 1930, and

- 1147 subsequent Burma earthquakes up to January, 1932. *Memoirs of the Geological Society of*
1148 *India*, **72**. Geological Survey of India, Calcutta, India.
- 1149 CONEY, P. J. & HARMS, T. A. 1984. Cordilleran metamorphic core complexes – Cenozoic extensional
1150 relics of Mesozoic compression. *Geology*, **12**, 550–554.
- 1151 COPLEY, A. & MCKENZIE, D. 2007. Models of crustal flow in the India-Asia collision zone.
1152 *Geophysical Journal International*, **169**, 683–698, doi: 10.1111/j.1365-246X.2007.03343.x.
- 1153 CURRAY, J. R. 2005. Tectonics and History of the Andaman Sea region. *Journal of Asian Earth*
1154 *Sciences*, **25**, 187–232.
- 1155 CURRAY, J. R., MOORE, D. G., LAWVER, L. A., EMMEL, F. J. & RAITT, R. W. 1979. Tectonics of the
1156 Andaman Sea and Burma. In: Watkins, J., Montadert, L & Dickenson, P. W. (eds) *Geological*
1157 *and Geophysical Investigations of Continental Margins*. American Association of Petroleum
1158 Geologists Memoir, **29**, 189–198.
- 1159 CURRAY, J. R., EMMEL, F. J., MOORE, D. G. & RAITT, R. W. 1982. Structure, tectonics and geological
1160 history of the northeastern Indian Ocean. In: NAIRN, A. E. M., & STEHLI, F. G. (eds.), *The*
1161 *Ocean Basins and Margins*. The Indian Ocean, **6**. Plenum Press, New York, 399–450.
- 1162 DE TERRA, H. 1943. The Pleistocene of Burma. *Transactions of the American Philosophical Society*,
1163 **64**, 271–340.
- 1164 DEPARTMENT OF POPULATION, MINISTRY OF IMMIGRATION AND POPULATION. 2015. The 2014 My-
1165 anmar Population and Housing Census: The Union Report. Census Report Volume 2:, Union
1166 of Myanmar, August 2014. 277 pp.
- 1167 DEY, B. P. 1968. Aerial photo interpretation of a major lineament in the Yamethin-Pyawbwe
1168 quadrangles. *Union of Burma Journal of Science and Technology*, **1**, 91–113.
- 1169 DOOLEY, T. & MCCLAY, K. R. 1997. Analogue modelling of pull-apart basins. *American Association*
1170 *of Petroleum Geologists Bulletin*, **81**, 1804–1826.
- 1171 DUMAN, T. Y., EMRE, O., DOGAN, A. & OZALP, S. 2005. Step-Over and Bend Structures along the
1172 1999 Duzce Earthquake Surface Rupture, North Anatolian Fault, Turkey. *Bulletin of the*
1173 *Seismological Society of America*, **95**, 1250–1262, doi: 10.1785/0120040082.
- 1174 ENGDAHL, E. R. & VILLASEÑOR, A. 2002. Global Seismicity: 1900–1999, International Handbook of
1175 Earthquake and Engineering Seismology, v. 81A, Elsevier Science Ltd., Amsterdam,
1176 Netherlands, 665–690.
- 1177 ENGLAND, P. & MOLNAR, P. 2005. Late Quaternary to decadal velocity fields in Asia. *Journal of*
1178 *Geophysical Research*, **110**, B12401, doi:10.1029/2004JB003541.
- 1179 EVERETT, J. R., RUSSEL, O. R., STASKOWSKI, R. J., LOYD, S. P., TABBUTT, V. M., DOLAN, P. & STEIN,
1180 A. 1990. Regional tectonics of Myanmar (Burma) and adjacent areas. Proceedings of the
1181 Seventh Thematic Conference on Remote Sensing for Exploration Geology, Calgary, Alberta,
1182 Canada, 651.
- 1183 GARDINER, N. J., SEARLE, M. P., ROBB, L. J. & MORLEY, C. K. 2015. Neo-Tethyan magmatism and
1184 metallogeny in Myanmar – An Andean analogue? *Journal of Asian Earth Sciences*. **106**. 197-
1185 215.
- 1186 GARSON, M. S., AMOS, B. J. & MITCHELL, A. H. G. 1976. The Geology of the country around
1187 Nyaunggya and Yengan, southern Shan states, Burma. Institute of Geological Sciences,
1188 Overseas Memoirs, 2, HMSO, London.
- 1189 GENÇ, Y. & YÜRÜR, M. T. 2010. Coeval extension and compression in Late Mesozoic-Recent thin-
1190 skinned extensional tectonics in central Anatolia, Turkey. *Journal of Structural Geology*, **32**,
1191 623–640.
- 1192 GRANT BROWN, R. 1911. The Tamans of the Upper Chindwin, Burma. *The Journal of the Royal*
1193 *Anthropological Institute of Great Britain and Ireland*, **41**, 305–317.
- 1194 GRAYMER, R. W., LANGENHEIM, V. E., SIMPSON, R. W., JACHENS, R. C. & PONCE, D. A. 2007.

- 1195 Relatively simple through-going fault planes at large-earthquake depth may be concealed by
 1196 surface complexity of strike-slip faults. In: CUNNINGHAM, W. D. & MANN, P. (eds) *Tectonics*
 1197 *of Strike-Slip Restraining and Releasing Bends*. Geological Society, London, Special
 1198 Publications, **290**, 189–201.
- 1199 GUTENBERG, B. & RICHTER, C. F. 1954. Seismicity of the Earth and Associated Phenomena. 2nd ed.,
 1200 Princeton University Press, Princeton, U.S.A. 310 pp.
- 1201 GUZMÁN-SPEZIALE, M. & NI, J. F. 1993. The opening of the Andaman Sea: Where is the short-term
 1202 displacement being taken up? *Geophysical Research Letters*, **20**, 2949–2952.
- 1203 GUZMÁN-SPEZIALE, M. & NI, J. F. 1996. Seismicity and active tectonics of the Western Sunda Arc. In:
 1204 Yin, A. & Harrison, T. M. (Eds.), *The Tectonic Evolution of Asia*, Cambridge University
 1205 Press, New York, pp. 63–84.
- 1206 HALL, R. 2002. Cenozoic geological and plate tectonic evolution of SE Asia and the SW Pacific:
 1207 computer-based reconstructions, model and animations. *Journal of Asian Earth Sciences*, **20**,
 1208 353–431.
- 1209 HALL, R. 2012. Late Jurassic–Cenozoic reconstructions of the Indonesian region and the Indian
 1210 Ocean. *Tectonophysics*, **570–571**, 1–41.
- 1211 HALL, R. & MORLEY, C. K. 2004. Sundaland Basins. *Continent-Ocean Interactions within East Asian*
 1212 *Marginal Seas. American Geophysical Union Geophysical Monograph Series*, **149**, 55–85.
- 1213 HARRISON, T. M., WENJI, C., LELOUP, P. H., RYERSON, F. J. & TAPPONNIER, P. 1992. An early Miocene
 1214 transition in deformation regime within the Red River fault zone, Yunnan, and its significance
 1215 for Indo-Asian tectonics. *Journal of Geophysical Research*, **97**, 7159–82.
- 1216 HLA HLA AUNG. 2011. Reinterpretation of historical earthquakes during 1929 to 1931. *Myanmar*
 1217 *Advances in Geosciences*, **31**, 43–57.
- 1218 HLA MAUNG. 1987. Transcurrent movements in the Burma–Andaman Sea region. *Geology*, **15**, 911–
 1219 912.
- 1220 HOLT, W. E., NI, J. F. WALLACE, T. C. & HAINES, A. J. 1991. The active tectonics of the eastern
 1221 Himalayan syntaxis and surrounding regions. *Journal of Geophysical Research*, **96**, 14,595–
 1222 14,632.
- 1223 HURUKAWA, N. & PHYO MAUNG MAUNG. 2011. Two seismic gaps on the Sagaing Fault, Myanmar,
 1224 derived from relocation of historical earthquakes since 1918. *Geophysical Research Letters*,
 1225 **38**, doi: 10.1029/2010GL046099.
- 1226 HUTCHISON, C. S. 1989. Geological Evolution of South-east Asia. Clarendon Press, Oxford. 368 pp.
- 1227 HUTCHISON, C. S. 1994. Gondwana and Cathaysian blocks, Palaeotethys sutures and Cenozoic
 1228 tectonics in South-East Asia. *Geologische Rundschau*, **82**, 388–405.
- 1229 KAMESH RAJU, K. A., RAMPRASAD, T., RAO, P.S., RAMALINGESWARA RAO, B. & JUBY VARGHESE.
 1230 2004. New insights into the tectonic evolution of the Andaman Basin, northeast Indian Ocean,
 1231 *Earth and Planetary Science Letters*, **221**, 145–162.
- 1232 KING, G. C. P. & WESNOUSKY, S. G. 2007. Scaling of fault parameters for continental strike-slip
 1233 earthquakes. *Bulletin of the Seismological Society of America*, **97**, 1833–1840.
- 1234 KO KO GYI, SAW HTWE ZAW, SOE THURA TUN, NYUNT HTAY, KYAW HTUN, MYO THANT, SOE MIN,
 1235 LIN THU AUNG, SHIKADA, M. & THINN HLAING OO, 2012. The 2012 Thabeikkyin
 1236 Earthquake. Situation Report 1 (121119), SEEDS Asia, 28 pp.
- 1237 KOSTROV, B.V. & DAS, S. 1988. Principles of Earthquake Source Mechanics. Cambridge University
 1238 Press, New York, USA. 286pp.
- 1239 KUNDU, B. & GAHALAUT, V. K. 2012. Earthquake occurrence processes in the Indo-Burmese wedge
 1240 and Sagaing fault region. *Tectonophysics*, **524–525**, 135–146.
- 1241 LA TOUCHÉ, T. H. D. 1913. The geology of the Northern Shan States. *Memoir of the Geological*
 1242 *Society of India*, **39**, 1–379.

- 1243 LACASSIN, R., MALUSKI, H., LELOUP, P. H., TAPPONNIER, P., HINTHONG, C., SIRIBHAKDI, K.,
1244 CHUAVIROJ, S. & CHAROENRAVAT, A. 1997. Tertiary diachronic extrusion and deformation of
1245 western Indochina: structure and $^{40}\text{Ar}/^{39}\text{Ar}$ evidence from NW Thailand. *Journal of*
1246 *Geophysical Research*, **102**, 10013-10037.
- 1247 LE DAIN, A. Y., TAPPONNIER, P. & MOLNAR, P. 1984. Active faulting and tectonics of Burma and
1248 surrounding regions. *Journal of Geophysical Research*, **89**, 453-472.
- 1249 LEE, H., CHUNG, S., YANG, H., CHU, C., LO, C. & MITCHELL, A. 2010. Cenozoic volcanic rocks from
1250 central Myanmar: Age, geochemical characteristics and geodynamic significance. American
1251 Geophysical Union, Fall Meeting 2010, abstract #T43B-2227.
- 1252 LELOUP, P. H., ARNAUD, N., LACASSIN, R., KIENAST, J. R., HARRISON, T. M., PHAN TRONG, T. T.,
1253 REPLUMAZ, A. & TAPPONNIER, P. 2001. New constraints on the structure, thermochronology,
1254 and timing of the Ailao Shan-Red River shear zone, SE Asia. *Journal of Geophysical*
1255 *Research*, **106**, 6683-6732.
- 1256 LELOUP, P. H., TAPPONNIER, P., LACASSIN, R. & SEARLE, M. P. 2007. Discussion on the role of the
1257 Red River shear zone, Yunnan and Vietnam, in the continental extrusion of SE Asia. *Journal*
1258 *of the Geological Society*, **164**, 1253-1260.
- 1259 LETTIS, W., BACHHUBER, J., WITTER, R., BRANKMAN, C., RANDOLPH, C. E., BARKA, A., PAGE, W. D.
1260 & KAYA, A. 2002. Influence of Releasing Step-Overs on Surface Fault Rupture and Fault
1261 Segmentation: Examples from the 17 August 1999 Izmit Earthquake on the North Anatolian
1262 Fault, Turkey. *Bulletin of the Seismological Society of America*, **92**, 19-42.
- 1263 LI, C., VAN DER HILST, R. D., MELTZER, A. S. & ENGDAHL, E. R. 2008. Subduction of the Indian litho-
1264 sphere beneath the Tibetan Plateau and Burma. *Earth and Planetary Science Letters*, **274**,
1265 157-168.
- 1266 LIN, A. & NISHIKAWA, M. 2011. Riedel shear structures in the co-seismic surface rupture zone
1267 produced by the 2001 M_w 7.8 Kunlun earthquake, northern Tibetan Plateau. *Journal of*
1268 *Structural Geology*, **33**, 1302-1311.
- 1269 LUO, Y., YU, H., ZHENG, Z.-J. & SHE, T. 2012. Regression analysis between environmental factors and
1270 earthquake-damaged trace: a case study in Wenchuan County, China. *International Journal of*
1271 *Remote Sensing*, **33**, 7088-7098.
- 1272 MACDONALD, A.S., BARR, S.M., DUNNING, G.R. & YAOWANOIYOTHIN, W. 1993, The Doi Inthanon
1273 metamorphic core complex in NW Thailand: age and tectonic significance. *Journal of*
1274 *Southeast Asian Earth Sciences*, **8**, 117-125.
- 1275 MANDL, G. 1988. *Mechanics of Tectonic Faulting*. Elsevier, Amsterdam, 408pp.
- 1276 MAURIN, T., MASSON, F., RANGIN, C., THAN MIN & COLLARD, P. 2010. First global positioning
1277 system results in northern Myanmar: constant and localized slip rate along the Sagaing Fault.
1278 *Geology*, **38**, 591-594.
- 1279 MCCAFFREY, R. 1996. Slip partitioning at convergent plate boundaries of SE Asia. In: Hall, R. &
1280 Blundell, D. J. (eds) *Tectonic Evolution of Southeast Asia*. Geological Society, London,
1281 Special Publications, **106**, 3-18.
- 1282 METCALFE, I. 1984. Stratigraphy, palaeontology and palaeogeography of the Carboniferous of
1283 Southeast Asia. *Memoirs of the Geological Society of France*, **147**, 107-118.
- 1284 METCALFE, I. 1996. Pre-Cretaceous evolution of SE Asian terranes. In: HALL, R., & BLUNDELL, D.,
1285 (eds), *Tectonic Evolution of Southeast Asia*, Geological Society Special Publications, **106**, 97-
1286 122.
- 1287 MITCHELL, A. H. G. 1977. Tectonic settings for emplacement of Southeast Asian tin granites.
1288 *Geological Society of Malaysia Bulletin*, **9**, 123-140.
- 1289 MITCHELL, A. H. G. 1981. Phanerozoic plate boundaries in mainland SE Asia, the Himalayas and
1290 Tibet. *Journal of the Geological Society*, **138**, 109-122.

- 1291 MITCHELL, A. H. G. 1992. Late Permian–Mesozoic events and the Mergui group Nappe in Myanmar
1292 and Thailand. *Journal of SE Asian Earth Sciences*, **7**, 165–178.
- 1293 MITCHELL, A. H. G. 1993. Cretaceous-Cenozoic tectonic events in the Western Myanmar (Burma)-
1294 Assam region. *Journal of the Geological Society, London*, **150**, 1089-1102.
- 1295 MITCHELL, A. H. G., HLAING, T. & HTAY, N. 2002. Mesozoic orogenies along the Mandalay-Yangon
1296 margin of the Shan Plateau. In: Montajit, N. (ed.), *Symposium on the Geology of Thailand*,
1297 26-31 August 2002, Bangkok, 136-149.
- 1298 MITCHELL, A. H. G., HTAY, M. T., HTUN, K. M., WIN, M. N., OO, T. & HLAING, T. 2007. Rock
1299 relationships in the Mogok metamorphic belt, Tatkon to Mandalay, central Myanmar. *Journal*
1300 *of Asian Earth Sciences*, **29**, 891–910.
- 1301 MITCHELL, A., CHUNG, S.-L., OO, T., LIN, T.-H. & HUNG, C.-H. 2012. Zircon U-Pb ages in Myanmar:
1302 Magmatic-metamorphic events and the closure of a neo-Tethys ocean? *Journal of Asian Earth*
1303 *Sciences*, **56**, 1-23.
- 1304 MOLNAR, P. & DAYEM, K. E. 2010. Major intracontinental strike-slip faults and contrasts in
1305 lithospheric length. *Geosphere*, **6**, 444-467.
- 1306 MOLNAR, P. & TAPPONNIER, P. 1975. Cenozoic tectonics of Asia: effects of a continental collision.
1307 *Science*, **189**, 419-426.
- 1308 MORLEY, C. K. 2002. A tectonic model for the Tertiary evolution of strike-slip faults and rift basins in
1309 SE Asia. *Tectonophysics*, **347**, 189-215.
- 1310 MORLEY, C. K. 2004. Nested strike-slip duplexes, and other evidence for Late Cretaceous-Palaeogene
1311 transpressional tectonics before and during India-Eurasia collision, in Thailand, Myanmar and
1312 Malaysia. *Journal of the Geological Society, London*, **161**, 799-812.
- 1313 MORLEY, C. K. 2012. Late Cretaceous–Early Palaeogene tectonic development of SE Asia. *Earth-*
1314 *Science Reviews*, **115**, 37–75.
- 1315 MORLEY, C. K. 2013. Discussion of tectonic models for Cenozoic strike-slip fault-affected continental
1316 margins of mainland SE Asia. *Journal of Asian Earth Sciences*, **76**, 137-151.
- 1317 MORLEY, C. K. & ALVEY, A. 2015. Is spreading prolonged, episodic or incipient in the Andaman Sea?
1318 Evidence from deepwater sedimentation. *Journal of Asian Earth Sciences*, **98**, 446-456.
- 1319 MORLEY, C. K., CHARUSIRI, P. & WATKINSON, I. M. 2011. Structural geology of Thailand during the
1320 Cenozoic. In: RIDD, M. F., BARBER, A. J., & CROW, M. J., (eds), *The Geology of Thailand*,
1321 Geological Society, London, Memoir, 273-334.
- 1322 MUKHOPADHYAY, M. & DASGUPTA, S. 1988. Deep structure and tectonics of the Burmese arc: con-
1323 straints from earthquake and gravity data. *Tectonophysics*, **149**, 299–322.
- 1324 MYANMAR GEOSCIENCES SOCIETY. 2014. Geological Map of Myanmar. 1:2,250,000 scale. Myanmar
1325 Geosciences Society, Yangon, Myanmar.
- 1326 MYINT THEIN. 2012. Alluvial Fans of Sagaing Area in central Myanmar and their bearing on the
1327 active tectonic activity of the Sagaing Fault. 12th Regional congress on Geology, Mineral and
1328 Energy Resources of Southeast Asia, GEOSEA 2012, Geological Society of Thailand,
1329 Bangkok, Thailand, p72.
- 1330 MYINT THEIN. 2016. Current tectonic activity along the Sagaing Fault (Myanmar) indicated by
1331 alluvial fans. In: Barber, A. J. Ridd, M. F., Khin Zaw & Rangin, C. (eds.). *Myanmar:*
1332 *Geology, Resources and Tectonics*. Geological Society, London, Memoirs, XXX-XXX.
- 1333 MYINT THEIN, KYAW TINT & KAN SAW. 1982. Geology of part of the eastern margin of the Central
1334 Burma belt between Sagaing and Tagaung. Research Titles, Geoscience Group, Policy
1335 Directing Committee on Research Projects, Burma. 259-303.
- 1336 MYINT THEIN, KAN SAW, AYE KO AUNG & KYAW TINT. 1987. Geology of the area between Tigyaing
1337 and Katha. *Research Titles*, Natural Science Research Group, Policy Directing Committee on
1338 Research Projects, Science and Technology Committee, Burma, 135-219.

- 1339 MYINT THEIN, KYAW TINT & AYE KO AUNG. 1991. On the lateral displacement of the Sagaing Fault.
1340 Georeports, 1 (1), 23-34. University of Mandalay, Burma.
- 1341 NIELSEN, C., CHAMOT-ROOKE, N. & RANGIN, C. 2004. From partial to full strain partitioning along
1342 the Indo-Burmese hyper-oblique subduction. *Marine Geology*, **209**, 303-327.
- 1343 NIU, Z., WANG, M., SUN, H., SUN, J., YOU, X., GAN, W., XUE, G., HAO, J., XIN, S., WANG, Y., WANG,
1344 Y. & LI, B. 2005. Contemporary velocity field of crustal movement of Chinese mainland from
1345 Global Positioning System measurements. *Chinese Science Bulletin*, **50**, 939-941.
- 1346 PIVNIK, D. A., NAHM, J., TUCKER, R. S., SMITH, G. O., NYEIN, K., NYUNT, M. & MAUNG P. H. 1998.
1347 Polyphase deformation in a fore-arc/back-arc basin, Salin subbasin, Myanmar (Burma).
1348 *American Association of Petroleum Geologists Bulletin*, **82**, 1837-1856.
- 1349 POLACHAN, S. & RACEY, A. 1994. Stratigraphy of the Mergui basin, Andaman Sea: Implications from
1350 petroleum exploration. *Journal of Petroleum Geology*, **17**, 373-406.
- 1351 RADHA KRISHNA, M. & SANU, T. D. 2000. Seismotectonics and rates of active crustal deformation in
1352 the Burmese arc and adjacent regions. *Journal of Geodynamics*, **30**, 401-421.
- 1353 RANGIN, C., WIN, M., SAN, L., WIN, N., MOURET, C., BERTRAND, C. & THE GIAC SCIENTIFIC PARTY.
1354 1999. Cenozoic pull-apart basins in central Myanmar: the trace of the path of India along the
1355 western margin of Sundaland. *Terra Abstracts*, **4**, 59.
- 1356 RANGIN, C., MAURIN, T. & MASSON, F. 2013. Combined effects of Eurasia/Sunda oblique conver-
1357 gence and East-Tibetan crustal flow on the active tectonics of Burma. *Journal of Asian Earth*
1358 *Sciences*, **76**, 185-194.
- 1359 REPLUMAZ, A. 1999. Reconstruction de la zone de collision Inde-Asie, Étude centrée sur l'Indochine,
1360 PhD thesis, Université Paris 7-IPG, Paris, France.
- 1361 REPLUMAZ, A. & TAPPONNIER, P. 2003. Reconstruction of the deformed collision zone between India
1362 and Asia by backward motion of lithospheric blocks. *Journal of Geophysical Research*, **108**,
1363 1-24.
- 1364 RHODES, B. P., CONEJO, R., BENCHAWAN, T., TITUS, S. & LAWSON, R. 2005. Palaeocurrents and
1365 provenance of the Mae Rim Formation, northern Thailand: implications for tectonic evolution
1366 of the Chiang Mai Basin. *Journal of the Geological Society, London*, **162**, 51-63,
1367 <http://dx.doi.org/10.1144/0016-764903-128>.
- 1368 RICHARD, P., NAYLOR, M. A. & KOOPMAN, A. 1995. Experimental models of strike-slip tectonics.
1369 *Petroleum Geoscience*, **1**, 71-80.
- 1370 RIDD, M. F. 1971. The Phuket Group of Peninsular Thailand. *Geological Magazine*, **108**, 445-446.
- 1371 RIDD, M. F. & WATKINSON, I. 2013. The Phuket-Slate Belt terrane: tectonic evolution and strike-slip
1372 emplacement of a major terrane on the Sundaland margin of Thailand and Myanmar.
1373 *Proceedings of the Geologists' Association*, **124**, 994-1010.
- 1374 ROBINSON, D. P., DAS, S. & SEARLE, M. P. 2010. Earthquake fault superhighways. *Tectonophysics*,
1375 **493**, 236-243.
- 1376 ROYDEN, L. 1996. Coupling and decoupling of crust and mantle in convergent orogens: Implications
1377 for strain partitioning in the crust. *Journal of Geophysical Research*, **101**, 17,679-17,705, doi:
1378 10.1029/96JB00951.
- 1379 SAHU, V. K., GAHALAUT, V. K., RAJPUT, S., CHADHA, R. K., LAISHRAM, S. S. & KUMAR, A. 2006.
1380 Crustal deformation in the Indo-Burmese arc region: implications from the Myanmar and
1381 Southeast Asia GPS measurements. *Current Science-Bangalore*, **90**, 1688.
- 1382 SCHOLZ, C. H. 2002. *The Mechanics of Earthquakes and Faulting*. Cambridge University Press,
1383 Cambridge, U.K. 471 pp.
- 1384 SEARLE, D. L. & BA THAN HAQ. 1964. The Mogok Belt of Burma and its relationship to the
1385 Himalayan Orogeny. *Proceedings of International Geological Congress*, **22**, 132-161.
- 1386 SEARLE, M. P. 2006. Role of the Red River Shear zone, Yunnan and Vietnam, in the continental

- 1387 extrusion of SE Asia. *Journal of the Geological Society, London*, **163**, 1025-1036.
- 1388 SEARLE, M. P. & MORLEY, C. K. 2011. Tectonic and thermal evolution of Thailand in the regional
1389 context of SE Asia. In: Ridd, M. F., Barber, A. J., & Crow, M. J., (eds) *The Geology of*
1390 *Thailand*, Geological Society, London, Memoir, 539-572.
- 1391 SEARLE, M. P., NOBLE, S.R., COTTLE, J.M., WATERS, D. J., MITCHELL, A. H. G., HLAING, T. &
1392 HORSTWOOD, M. S. A. 2007. Tectonic evolution of the Mogok metamorphic belt, Burma
1393 (Myanmar) constrained by U-Th-Pb dating of metamorphic and magmatic rocks. *Tectonics*,
1394 **26**, TC3014, doi: 1029/2006TC002083.
- 1395 SEVASTJANOVA, I., HALL, R., RITTNER, M., PAW, S. M. T. L., NAING, T. T., ALDERTON, D. & COMFORT,
1396 G. 2015. Myanmar and Asia united, Australia left behind long ago. *Gondwana Research*.
1397 doi:10.1016/j.gr.2015.02.001.
- 1398 SLOAN, R.A., ELLIOTT, J.R., SEARLE, M.P. & MORLEY, C.K. 2016. Active Tectonics of Burma
1399 (Myanmar). In: Barber, A. J. Ridd, M. F., Khin Zaw & Rangin, C. (eds.). *Myanmar: Geology,*
1400 *Resources and Tectonics*. Geological Society, London, Memoirs, XXX-XXX.
- 1401 SOCQUET, A. & PUBELLIER, M. 2005. Cenozoic deformation in western Yunnan (China-Myanmar
1402 border). *Journal of Asian Earth Sciences*, **24**, 495-515.
- 1403 SOCQUET, A., VIGNY, C. CHAMOT-ROOKE, N., SIMONS, W., RANGIN, C. & AMBROSIUS, B. 2006. India
1404 and Sunda plates motion and deformation along their boundary in Myanmar determined by
1405 GPS. *Journal of Geophysical Research*, **111**. doi:10.1029/2005JB003877.
- 1406 SOE MIN, SOE THURA TUN, WATKINSON, I. M. & WIN NAING. 2016. The Kyaukkyan Fault. In: Barber,
1407 A. J. Ridd, M. F., Khin Zaw & Rangin, C. (eds.). *Myanmar: Geology, Resources and*
1408 *Tectonics*. Geological Society, London, Memoir, XXX-XXX.
- 1409 SOE THURA TUN. 1999. Mineralogical aspects of precious metals occurrence and geology of the
1410 Indawgyi area, Mohnyin Township, Myitkyina District. Unpublished MSc Thesis, University
1411 of Yangon, 129pp
- 1412 SOE THURA TUN & MAUNG THEIN. 2012. Tectonic map of Myanmar. Myanmar Geosciences Society,
1413 Yangon, Myanmar.
- 1414 SOE THURA TUN, WANG YU, SAW NGWE KHAING, MYO THANT, NYUNT HTAY, YIN MYO MIN HTWE,
1415 THAN MYINT & SIEH, K. 2014. Surface ruptures of the M_w 6.8 March 2011 Tarlay earthquake,
1416 eastern Myanmar. *Bulletin of the Seismological Society of America*, **104**, 2915-2932. doi:
1417 10.1785/0120130321.
- 1418 SPYROPOULOS, C., GRIFFITH, W. J., SCHOLZ, C. H. & SHAW, B. E. 1999. Experimental evidence for
1419 different strain regimes of crack populations in a clay model. *Geophysical Research Letters*,
1420 **26**, 1081-1084.
- 1421 SRISURIYON, K. & MORLEY, C. K. 2014. Pull-apart development at overlapping fault tips: Oblique
1422 rifting of a Cenozoic continental margin, northern Mergui Basin, Andaman Sea. *Geosphere*,
1423 **10**, 80-106. doi:10.1130/GES00926.1.
- 1424 STEPHENSON, D. & MARSHALL, T. R. 1984. The petrology and mineralogy of Mt. Popa volcano and
1425 the nature of the late Cenozoic Burma volcanic arc. *Journal of the Geological Society of*
1426 *London*, **141**, 747-762.
- 1427 STIRLING, M. W., WESNOUSKY, S. G. & SHIMAZAKI, K. 1996. Fault trace complexity, cumulative slip,
1428 and the shape of the magnitude-frequency distribution for strike-slip faults: A global survey.
1429 *Geophysical Journal International*. **124**, 833-868.
- 1430 TAPPONNIER, P., PELTZER, G., LE DAIN, A. Y., ARMIJO, R. & COBBOLD, P. 1982. Propagating extrusion
1431 tectonics in Asia: New insights from simple experiments with plasticine. *Geology*, **10**, 611-
1432 616.
- 1433 TAPPONNIER, P., PELTZER, G. & ARMIJO, R. 1986. On the mechanism of the collision between India
1434 and Asia. In: COWARD, M. P., & RIES, A. C. (eds.), *Collision Tectonics*, Geological Society,

- 1435 London, Special Publications, **19**, 115-157.
- 1436 TORRES, C., SWAUGER, D. A., BERGMAN, S., TAPPONNIER, P., LACASSIN, R. & REPLUMAZ, A. 1997.
- 1437 The Sagaing Fault in Myanmar: Preliminary field observations and relevance to the Gulf of
- 1438 Martaban Cenozoic Petroleum System. In: Howes, J. V. C. & Noble, R. A. (eds.), *Proceedings*
- 1439 *of the Petroleum Systems of SE Asia and Australasia Conference 1997, Indonesian Petroleum*
- 1440 *Association*, **335**.
- 1441 TRANSPARENCY INTERNATIONAL. 2014. Corruption Perceptions Index 2014: Results. World Wide
- 1442 Web Address: <http://www.transparency.org/cpi2014/results>.
- 1443 TRELOAR, P. J. & COWARD, M. P. 1991. Plate motion and shape: constraints on the geometry of the
- 1444 Himalayan orogen. *Tectonophysics*, **191**, 189–198.
- 1445 TREVENA, A. S., VARGA, R. J., COLLINS, I. D. & NU, U. 1991. Tertiary tectonics and sedimentation in
- 1446 the Salin (fore-arc) basin, Myanmar (abstract). *AAPG Bulletin*, **75**, 683.
- 1447 TSUTSUMI, H. & SATO, T. 2009. Tectonic geomorphology of the Southernmost Sagaing Fault and
- 1448 surface rupture associated with the May 1930 Pegu (Bago) Earthquake, Myanmar. *Bulletin of*
- 1449 *the Seismological Society of America*, **99**, 2155–2168. doi:10.1785/0120080113.
- 1450 UTKUCU, M., NALBANT, S. S., MCCLOSKEY, J., STEACY, S. & ALPTEKIN, O. 2003. Slip distribution
- 1451 and stress changes associated with the 1999 November 12, Düzce (Turkey) earthquake ($M_w =$
- 1452 7.1). *Geophysical Journal International*, **153**, 229-241.
- 1453 VAN HINSBERGEN, D. J. J., KAPP, P., DUPONT-NIVET, G., LIPPERT, P. C., DECELLES, P. G. & TORSVIK,
- 1454 T. H. 2011. Restoration of Cenozoic deformation in Asia and the size of Greater India.
- 1455 *Tectonics*, **30**, TC5003. <http://dx.doi.org/10.1029/2011TC002908>.
- 1456 VIGNY, C., SOCQUET, A., RANGIN, C., CHAMOT-ROOKE, N., PUBELLIER, M., BOUIN, M. -N.,
- 1457 BERTRAND, G. & BECKER, M. 2003. Present-day crustal deformation around the Sagaing
- 1458 fault, Myanmar. *Journal of Geophysical Research*, **108**, doi: 10.1029/2002JB001999.
- 1459 WALLACE, R. E. 1968. Notes on stream channels offset by the San Andreas fault. In: DICKINSON, W.
- 1460 R., & GRANTZ, A. (eds), *Conference on Geologic Problems of the San Andreas Fault System,*
- 1461 *Proceedings*, **11**, Stanford University Publications in the Geological Sciences, 6-21.
- 1462 WANG, E. & BURCHFIEL, B. C. 1997. Interpretation of Cenozoic tectonics in the right-lateral
- 1463 accommodation zone between the Ailao Shan shear zone and the eastern Himalayan syntaxis.
- 1464 *International Geology Review*, **39**, 191–219.
- 1465 WANG, P.-L., LO, C.-H., CHUNG, S.-L., LEE, T.-Y., LAN, C.-Y. & THANG, T. V. 2000. Onset timing of
- 1466 left-lateral movement along the Ailao Shan–Red River shear zone: $^{40}\text{Ar}/^{39}\text{Ar}$ dating
- 1467 constraint from the Nam Dinh area, northeastern Vietnam. *Journal of Asian Earth Sciences*,
- 1468 **18**, 281–292.
- 1469 WANG, Y., SIEH, K., THURA AUNG, SOE MIN, SAW NGWE KHAING & SOE THURA TUN. 2011.
- 1470 Earthquakes and slip rate of the southern Sagaing fault: insights from an offset ancient fort
- 1471 wall, lower Burma (Myanmar). *Geophysical Journal International*, **185**, 49-64.
- 1472 WANG, Y., SIEH, K., SOE THURA TUN, LAI, K.-Y. & THAN MYINT. 2014. Active tectonics and
- 1473 earthquake potential of the Myanmar region. *Journal of Geophysical Research: Solid Earth*,
- 1474 **119**, 3767-3822. doi:10.1002/2013JB010762.
- 1475 WATKINSON, I., ELDERS, C., BATT, G., JOURDAN, F., HALL, R. & MCNAUGHTON, N. J. 2011. The
- 1476 timing of strike–slip shear along the Ranong and Khlong Marui faults, Thailand. *Journal of*
- 1477 *Geophysical Research*, **116**. <http://dx.doi.org/10.1029/2011JB008379>.
- 1478 WELLS, D. L. & COPPERSMITH, K. J. 1994. New empirical relationships among magnitude, rupture
- 1479 length, rupture width, rupture area, and surface displacement. *Bulletin of the Seismological*
- 1480 *Society of America*, **84**, 974-1002.
- 1481 WERNICKE, B. P., CHRISTIANSEN, R. L., ENGLAND, P. C. & SONDER, L. J. 1987. Tectonomagmatic
- 1482 evolution of Cenozoic extension in the North American Cordillera. In: COWARD, M. P.,

- 1483 DEWEY, J. F., & HANCOCK, P. L. (eds.), *Continental Extensional Tectonics*. Geological Society
 1484 Special Publication, **28**, 203-221.
- 1485 WESNOUSKY, S. G. 1988. Seismological and structural evolution of strike-slip faults, *Nature*, **335**,
 1486 340–342.
- 1487 WESNOUSKY, S. G. 2006. Predicting the endpoints of earthquake ruptures. *Nature*. **444**, 358-360.
- 1488 WHITNEY, D. L., TEYSSIER, C., REY, P. & BUCK, R. 2013. Continental and oceanic core complexes.
 1489 *Geological Society of America Bulletin*, **125**, 273-298.
- 1490 WHITTAKER, J. M., MÜLLER, R. D., SDROLIAS, M. & HEINE, C. 2007. Sunda-Java trench kinematics,
 1491 slab window formation and overriding plate deformation since the Cretaceous. *Earth and*
 1492 *Planetary Science Letters*, **255**, 445–457.
- 1493 WIN SWE. 1970. Rift-features at the Sagaing-Tagaung ridge. Proceedings of the 5th Burma Research
 1494 Congress, Rangoon.
- 1495 WIN SWE. 1972. Strike-slip faulting in Central Belt of Burma (abstract). In: Haile, N. E. (ed),
 1496 *Regional Conference on the Geology of Southeast Asia*. Geological Society of Malaysia.
- 1497 WIN SWE. 2011. Earthquakes and related hazards in Myanmar. *Journal of the Myanmar Geosciences*
 1498 *Society*, **4**, 1-32.
- 1499 WIN SWE. 2012. Outline geology and economic mineral occurrences of the union of Myanmar.
 1500 *Journal of the Myanmar Geosciences Society, Special Publication*, **1**, 215 pp.
- 1501 WIN SWE. 2013. The Sagaing Fault of Myanmar: A brief overview. Geology of Sagaing Fault, in
 1502 commemoration of 9th anniversary of MGS. Myanmar Geosciences Society, Yangon,
 1503 Myanmar.
- 1504 WYSS, M. 2005. Human losses expected in Himalayan earthquakes. *Natural Hazards*, **34**, 305-314.
- 1505 YEATS, R. 2012. Active Faults of the World. Cambridge University Press, Cambridge, U.K. 621 pp.
- 1506 YEATS, R. S., SIEH, K. & ALLEN, C. R. 1997. The Geology of Earthquakes. Oxford University Press,
 1507 Oxford, 568 pp.
- 1508 ZHANG, B., ZHANG, J., ZHONG, D., YANG, L., YUE, Y. & YAN, S. 2012. Polystage deformation of the
 1509 Gaoligong metamorphic zone: Structures, 40Ar/39Ar mica ages, and tectonic implications.
 1510 *Journal of Structural Geology*, **37**, 1-18.
- 1511 ZHANG, L-S. & SCHARER, U. 1999. Age and origin of magmatism along the Cenozoic Red River shear
 1512 belt, China. *Contributions to Mineralogy and Petrology*, **134**, 67-85.

1513 **Figure and table captions**

1514 **Fig. 1:** Tectonic setting of the Sagaing Fault. Modified after Morley *et al.* (2011); Soe Thura Tun &
 1515 Maung Thein (2012); Wang *et al.* (2014); Morley & Alvey (2015).

1516 **Fig 2:** Overview maps of the onshore Sagaing Fault. a) Topography, geomorphic and structural
 1517 elements of the Sagaing Fault. Segments modified after Wang *et al.* (2014). Digital elevation model
 1518 basemap constructed from ASTER GDEM. ASTER GDEM is a product of METI and NASA.
 1519 Yellows, browns and whites are elevations >400 m. Greens and blues are lower elevations. For
 1520 location see Fig. 1. b) Geology along the Sagaing Fault. Geology modified after Myanmar
 1521 Geosciences Society (2014). c) Seismicity along the Sagaing Fault. Earthquake hypocentres (red)
 1522 1970-2015 with depths <50 km from USGS compilation
 1523 (<http://earthquake.usgs.gov/earthquakes/search/>). Focal mechanisms for selected events from the
 1524 CMT catalogue plotted using Mirone software. Relocated earthquake locations (blue) from Hurukawa
 1525 & Phyo Maung Maung (2011) and (*) from Wang *et al.* 2014. Rupture extent for main historic
 1526 earthquakes modified after Wang *et al.* (2014). Deeper colours are more recent. Dashed lines indicate
 1527 uncertainty. Line thickness is set for the purpose of clarity only.

1528 **Fig. 3:** Landsat ETM+ mosaic (bands 742) of the Sagaing Fault, showing the main geomorphic
 1529 domains. Main trace of the Sagaing Fault is highlighted in white. Soils and thin vegetation appears
 1530 grey, pink and purple. Thick vegetation appears deep green.

1531 **Fig. 4:** Tectonic geomorphology of the Sagaing Fault. For locations see Fig. 3. a) Low relief and
 1532 subtle pressure ridges south of Bago. b) Growing fold adjacent to the Meiktila segment. Brown lines
 1533 indicate dry streams, blue lines indicate active rivers. See text for details. Basemap constructed from
 1534 ASTER GDEM. c) Triangular facets marking a strand of the Sagaing Fault on the east bank of the
 1535 Ayeyarwaddy River south of Sabeanago. Image taken in April 2013, most of the facets have been
 1536 stripped by landslides during the November 2012 earthquake. d) Dry gully showing a cumulative
 1537 1.75 m offset caused by 2012 and 1946 earthquakes. e) Possible palaeoseismic scarp in alluvial fans at
 1538 the foot of the main Sagaing Ridge. Note stream erosion and partial collapse of the scarp.

1539 **Fig. 5:** Satellite imagery of Sagaing Fault geomorphology. For locations see Fig. 3. a) Remarkably
 1540 linear trace of the fault across deltaic sediments immediately north of the Gulf of Mottama. Imagery
 1541 from the ERSI Global Imagery database and sources therein. b) Landsat ETM+ image of the Pyu
 1542 segment (bands 451 with panchromatic sharpening) draped over ASTER DEM. Streams (blue) picked
 1543 as they cross main faults. Wet soils appear blue, dry soils appear green, dense vegetation is red. c)
 1544 Lineaments defined by sandbanks in the Ayeyarwaddy River between Male and Sabeanago,
 1545 highlighting Sagaing Fault strands and vertical motions. Imagery from the ERSI Global Imagery
 1546 database and sources therein.

1547 **Fig. 6:** Examples of pressure ridges along the Sagaing segment. a) Small coseismic pressure ridge
 1548 defined by Riedel shears and thrust faults, formed north of Singu during the 2012 earthquake. b) Pre-
 1549 existing pressure ridge within a fault-bounded valley north of Thabeikkyin, amplified by the 2012
 1550 earthquake. c) One of a number of parallel and en-echelon ridges exposing Irrawaddy Gp. strata north
 1551 of Singu. d) Steep-sided shutter ridge exposing tectonised amphibolites close to the western margin of
 1552 the Shan Plateau. e) Representative of the highly linear, symmetric pressure ridges lining the
 1553 Ayeyarwaddy River along the northern half of the Sagaing segment. f) View along Sagaing Ridge,
 1554 showing the steeper western flank and more shallow eastern flank.

1555 **Fig 7:** Overview map showing topographic, geomorphic and structural elements of the northern
 1556 termination and transform system. Faults modified after Morley *et al.* (2011); Soe Thura Tun &
 1557 Maung Thein (2012); Wang *et al.* (2014). Segments modified after Wang *et al.* (2014). Digital
 1558 elevation model basemap constructed from ASTER GDEM. Greys, browns and pinks are elevations
 1559 >300 m. Greens and blues are lower elevations. For location see Fig. 1.

1560 **Fig. 8:** Details of fault complexities along the northern Sagaing Fault, mapped using ASTER GDEM,
 1561 Landsat ETM+ and ERSI Global Imagery (except d, surveyed on the ground). For locations see Fig.
 1562 3. a) Ban Mauk segment and horsetail splay. b) Indaw Lake step-over basin. c) Strike-slip splays and
 1563 extensional systems around Indawgyi Lake. d) Coseismic fractures revealing small step-over and zone
 1564 of subsidence formed during the 2012 earthquake.

1565 **Fig. 9:** Details of fault complexities along the southern Sagaing Fault, mapped using ASTER GDEM,
 1566 Landsat ETM+ and ERSI Global Imagery and incorporating field observations. For locations see Fig.
 1567 3. a) Singu basalt plateau showing the southern termination of the 2012 surface rupture. b) Sagaing
 1568 Ridge, showing Yega In and fault segmentation along the western margin. c) Nay Pyi Taw double
 1569 bend system. d) Restraining step-over between the Pyu and Bago segments.

1570 **Fig. 10:** Large-scale offset piercing points along the Sagaing Fault. a) Restoration of 340 km
 1571 displacement along the Sagaing Fault to bring the upper Chindwin into continuity with the
 1572 Ayeyarwaddy River. After Hla Maung (1987). b) Present-day arrangement of the Chindwin and
 1573 Ayeyarwaddy, showing the assumed piercing points used for the restoration in a). c) 203 km
 1574 displacement along the Sagaing Fault based on restoration of the Mayathein and Sagaing
 1575 metamorphics, presently exposed on the west and east sides of the fault respectively. After Myint
 1576 Thein *et al.* (1991).

1577 **Fig. 11:** Smaller-scale offset piercing points along the Sagaing Fault. a) Present-day outline of the
 1578 Pleistocene Singu basalt straddling the Sagaing Fault. b) Restoration of 2.7 km offset using the
 1579 southern margin of the basalt (yellow points). c) Restoration of 6.5 km offset using the northern
 1580 margin of the basalt (red points). After Bertrand *et al.* (1998). d) Displacement and capture of streams
 1581 crossing the Sagaing Fault south of Thabeikkyin. Solid blue lines are modern rivers, dashed lines are
 1582 abandoned channels. Blue arrows show flow direction. Deltas marked in brown. Faults based on field
 1583 mapping of the 2012 surface rupture. See text for explanation.

1584 **Fig. 12:** GPS vectors from all published surveys within Myanmar and around the eastern Himalayan
 1585 syntaxis. After Maurin *et al.* (2010). Stations referred to in the text are marked as yellow triangles.

1586 **Fig. 13:** Effects of earthquakes along the Sagaing Fault. a) Mingun Pagoda on the east side of Sagaing
 1587 Ridge, a solid brick construction damaged during the 1839 Amarapura earthquake. b) Thein Taung
 1588 pagoda, built on a pressure ridge south of Sabeanago, damaged during the 2012 Thabeikkyin
 1589 earthquake. c) Typical expression of the 2012 surface rupture, showing well-developed Riedel shears
 1590 and a component of down-dip extension.

1591 **Fig. 14:** Schematic evolutionary maps showing the development of the Sagaing Fault since Late
 1592 Eocene times, synthesised largely from ideas presented in Pivnik *et al.* (1998); Bertrand & Rangin
 1593 (2003); Socquet & Pubellier (2005); Morley *et al.* (2011); Searle & Morley (2011); Morley & Alvey
 1594 (2015). See text for explanation and additional references. Shows progressive westwards migration
 1595 and replacement by discrete strike-slip structures of a broad zone of dextral shear extending from the
 1596 southeastern Shan Plateau to the Gaoligong Shan and beyond. Major change from broadly NNW-SSE
 1597 directed extension to NE-SW compression (Socquet & Rangin 2005) coincides with the localisation
 1598 of the Sagaing Fault, basin inversion, cessation of subduction and cessation of metamorphic complex
 1599 exhumation. No attempt is made to show finite displacement across the fault systems because of the
 1600 large uncertainty involved. The modern coastline is for reference only.

1601 **Fig. 15:** The disparity between surface fault traces and 3-D geometry of strike-slip faults. a) Simple,
 1602 through-going fault in seismogenic basement splays upwards into 'cover' units, which may be
 1603 Quaternary drift deformed by coseismic fractures, or at a different scale the uppermost layers of rock.
 1604 Surface trace shows complex splay patterns defined by Riedel (R) and antithetic Riedel (R') shears,
 1605 synthetic P-shears and through-going Y-shears, together with areas of uplift and subsidence both
 1606 within strands and at step-overs. Adapted after Lin & Nishikawa (2011). b) Example of upward-
 1607 splaying from an inferred single lower fault strand of the Sagaing Fault observed in a quarry wall.
 1608 Coseismic fractures in Quaternary sands and silts north of Singu, formed during the 2012 Thabeikkyin
 1609 earthquake.

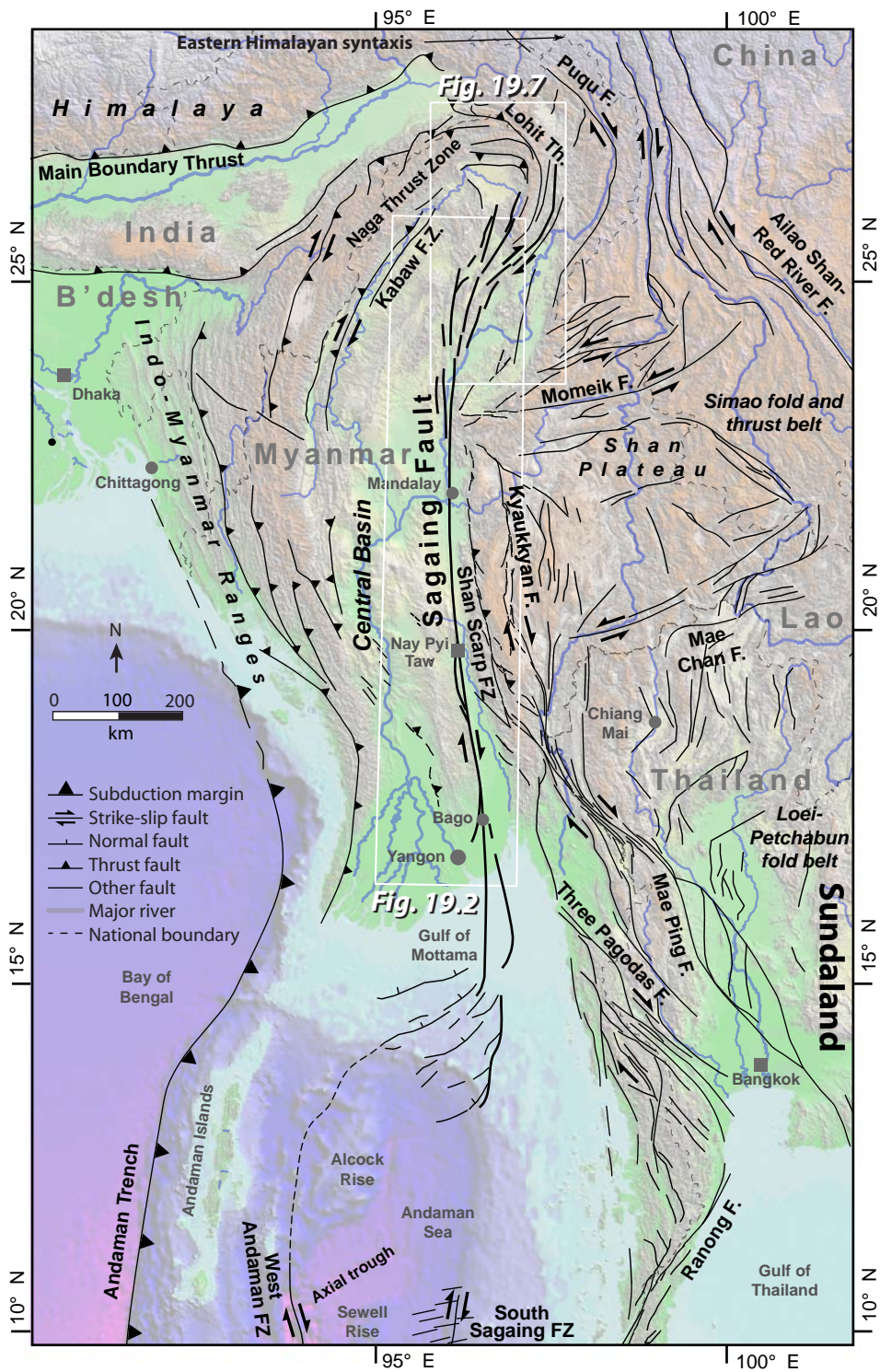


Fig. 19.1

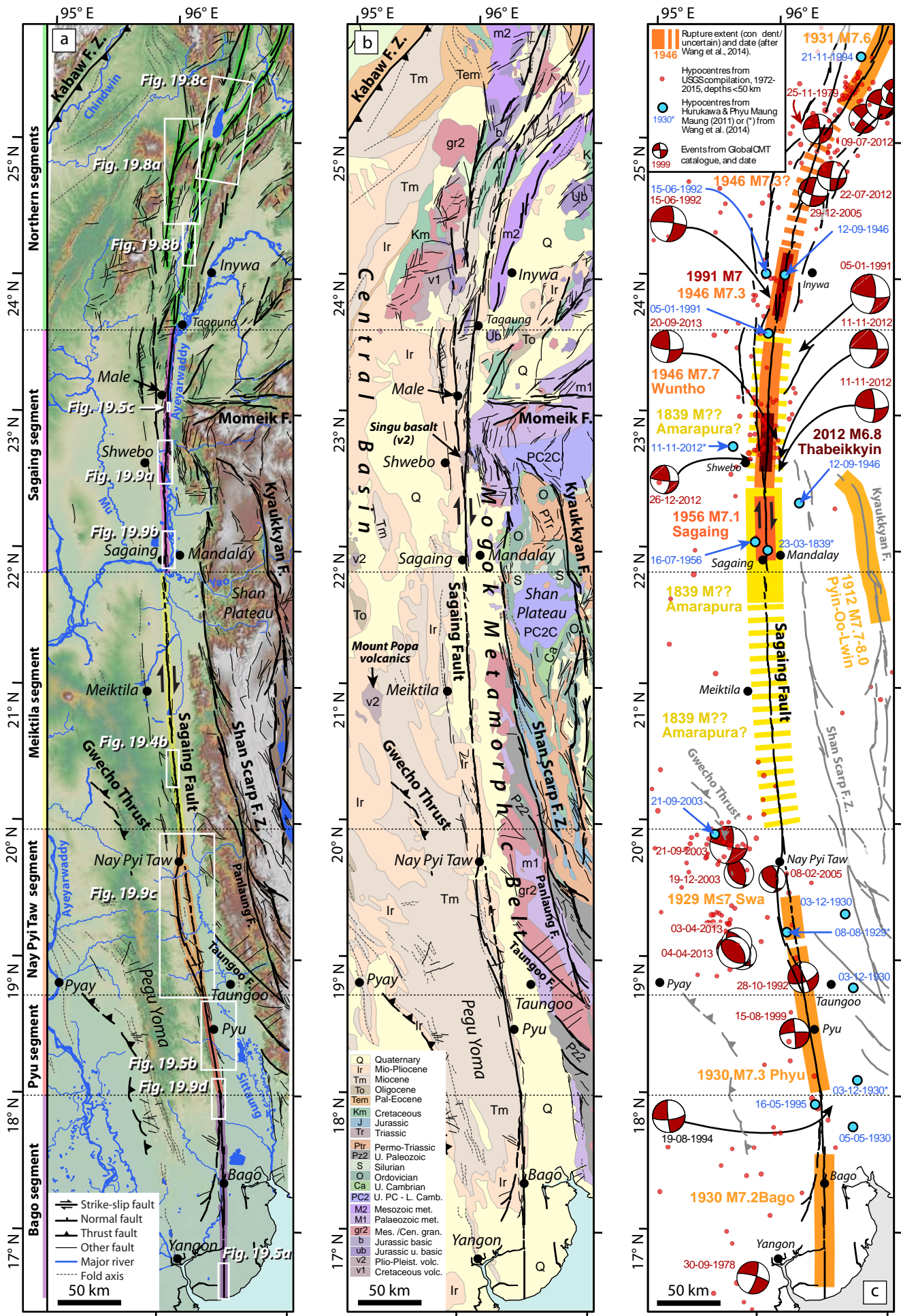


Fig. 19.2

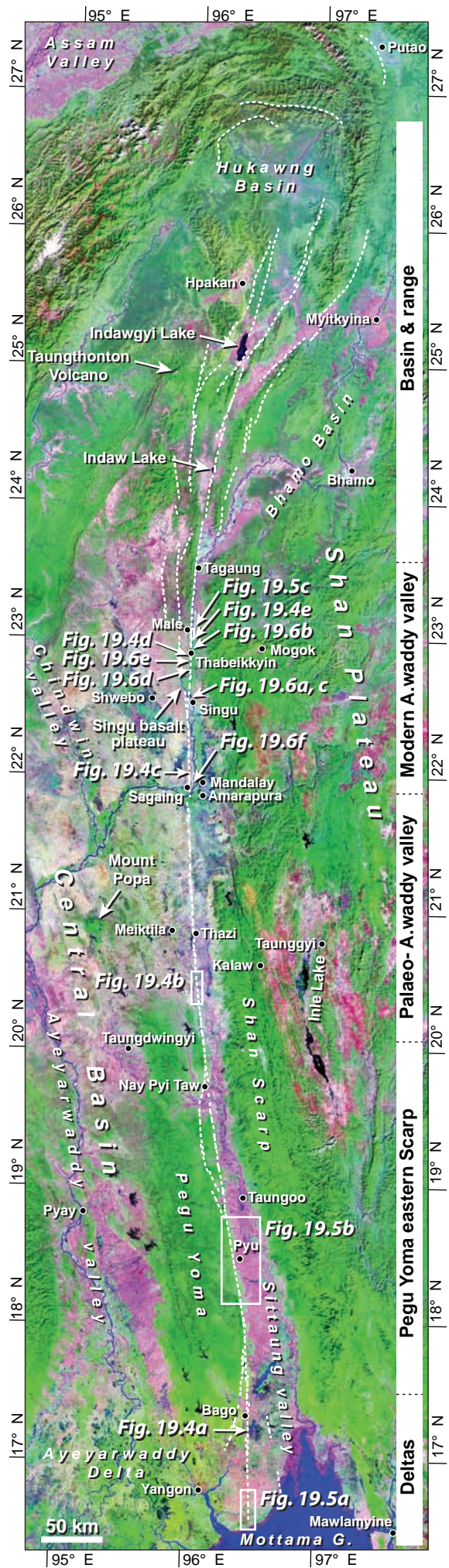


Fig. 19.3

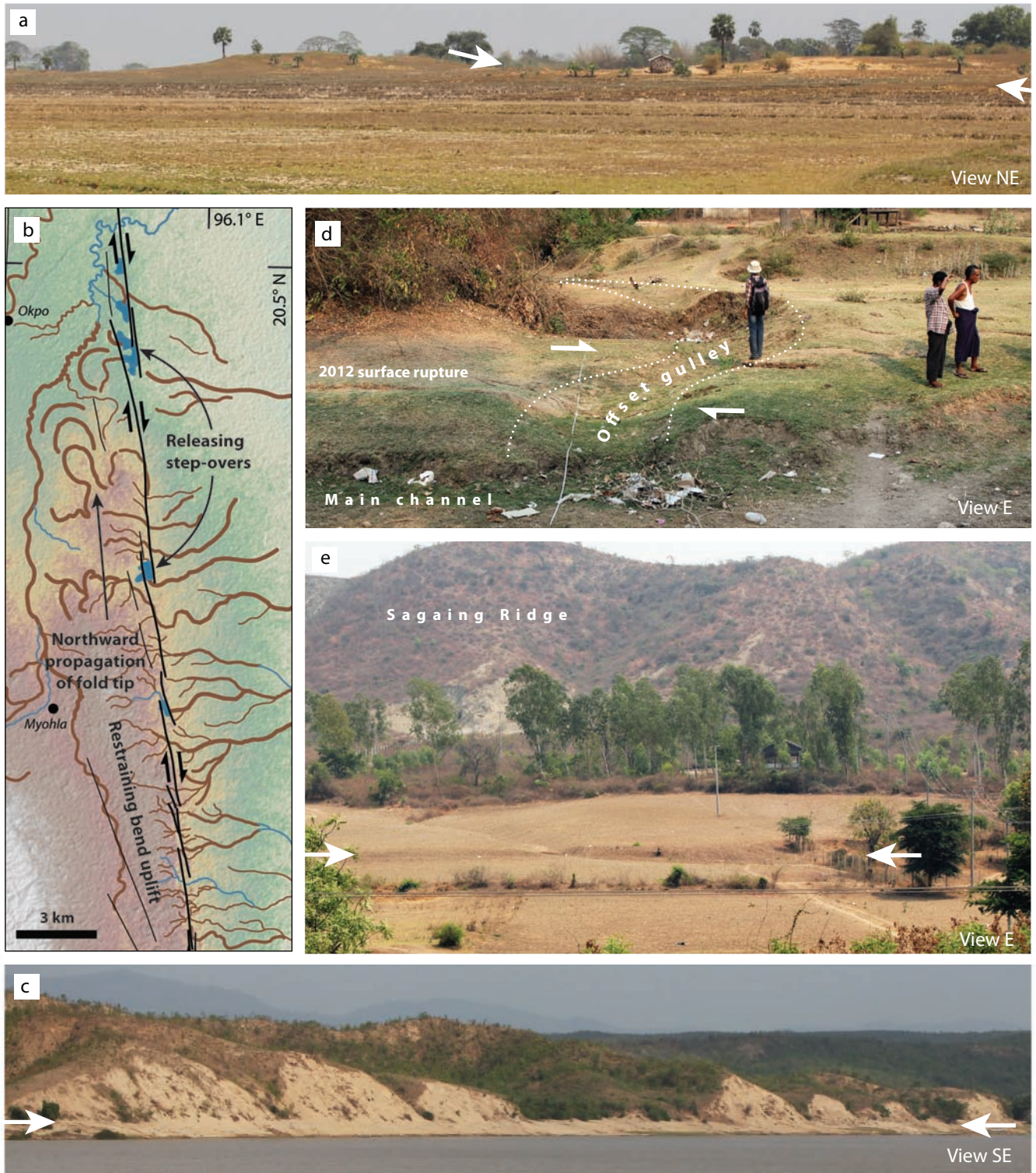


Fig. 19.4

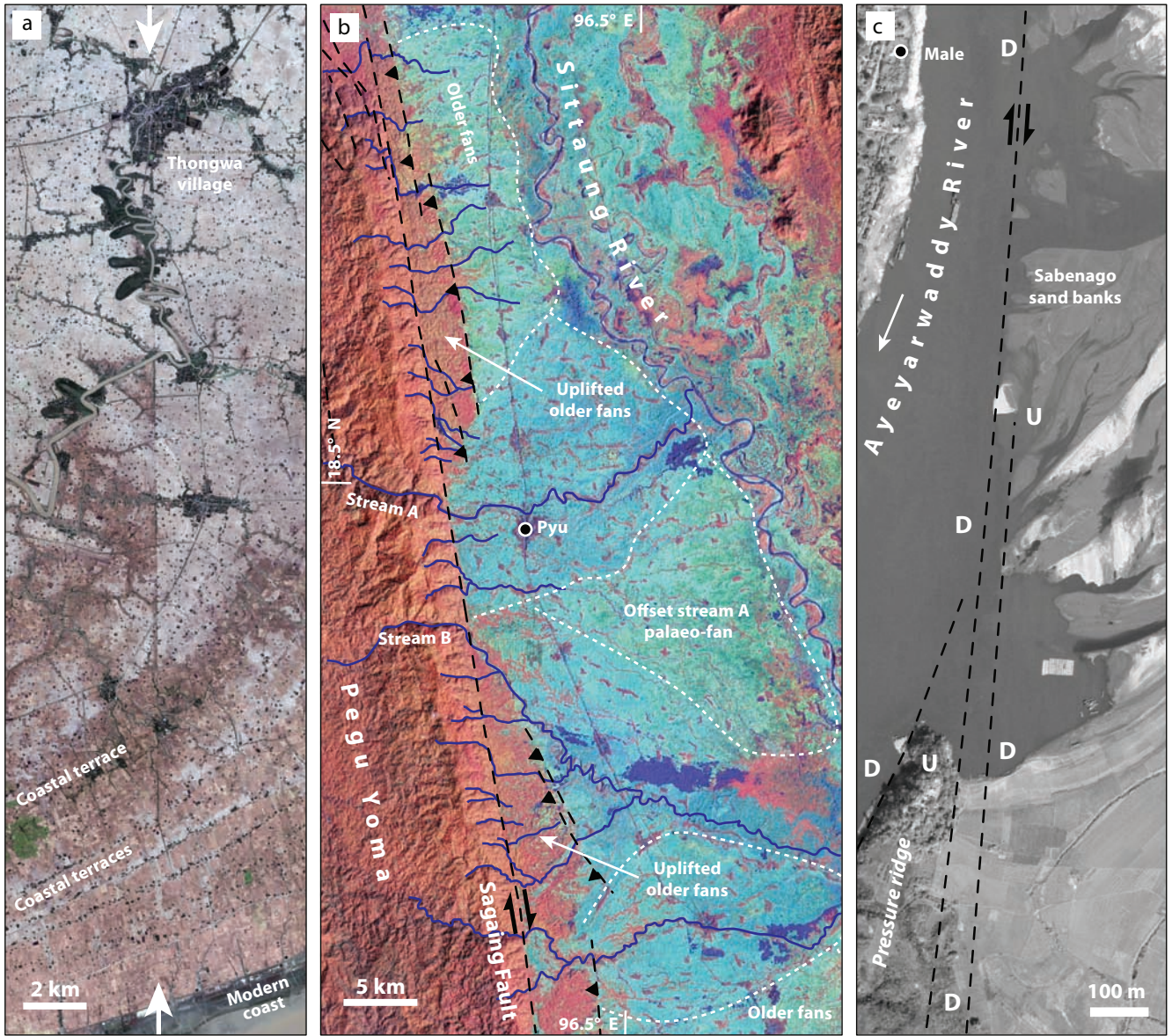


Fig. 19.5

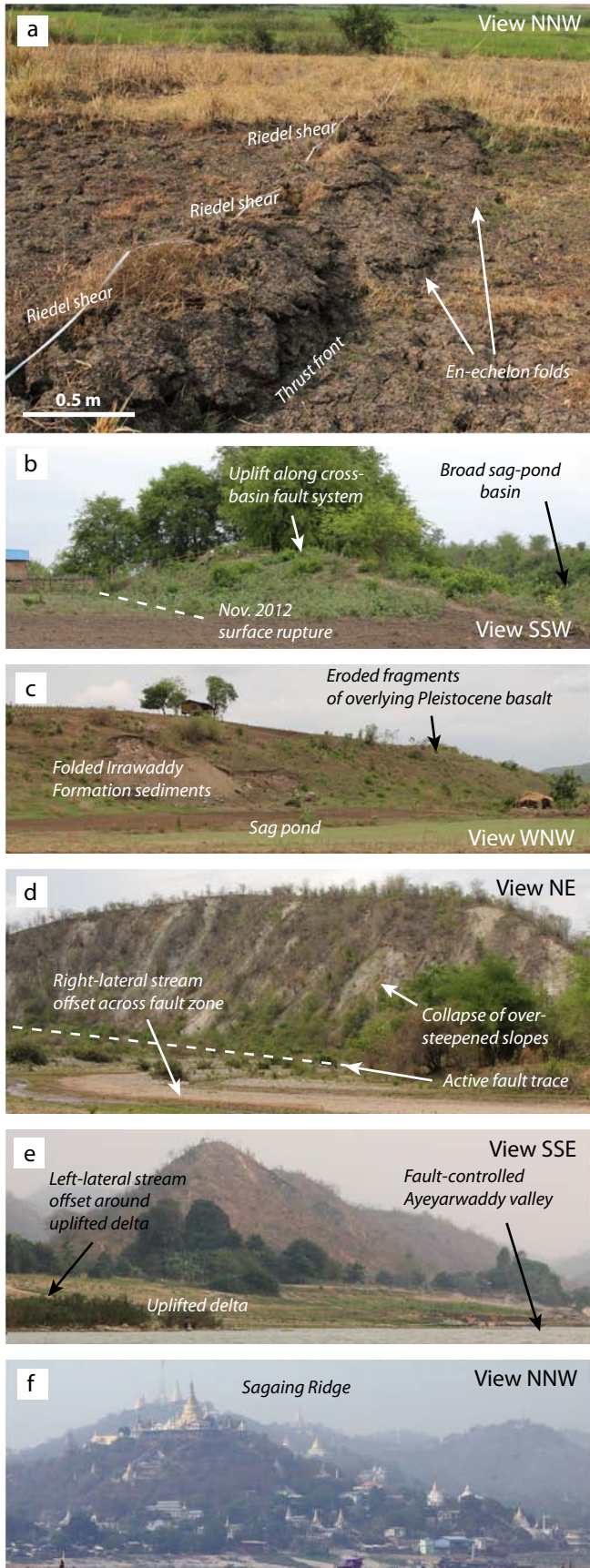


Fig. 19.6

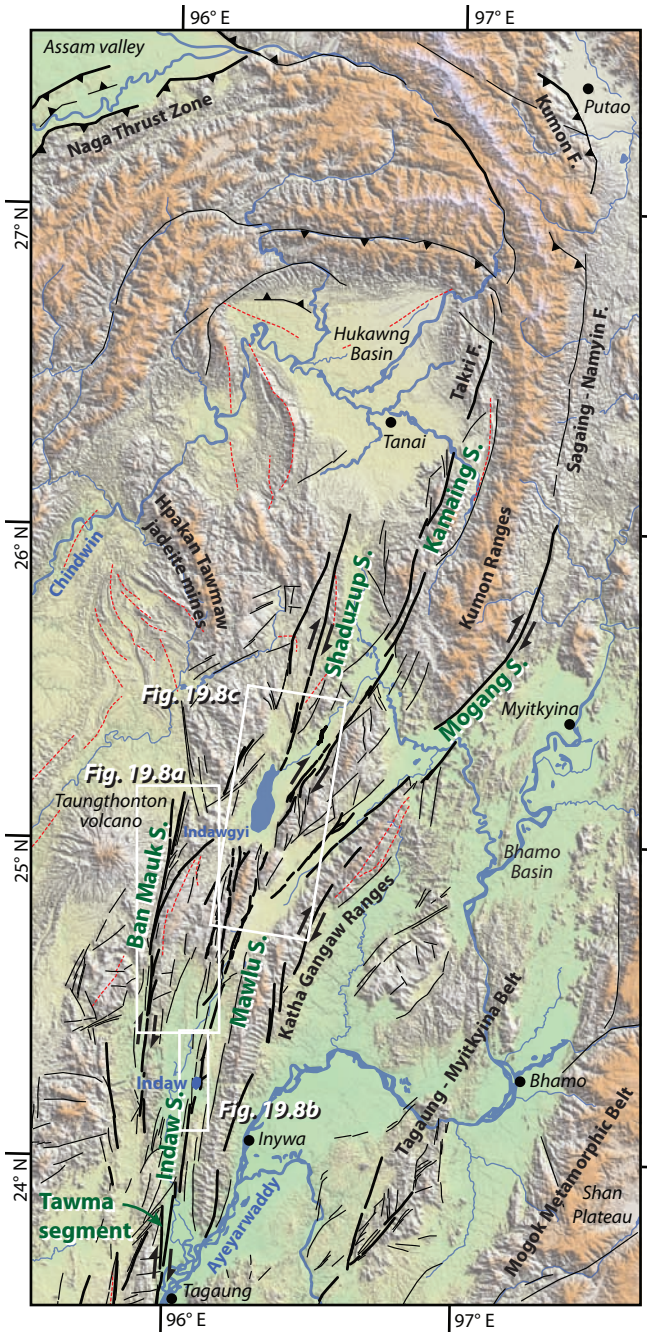


Fig. 19.7

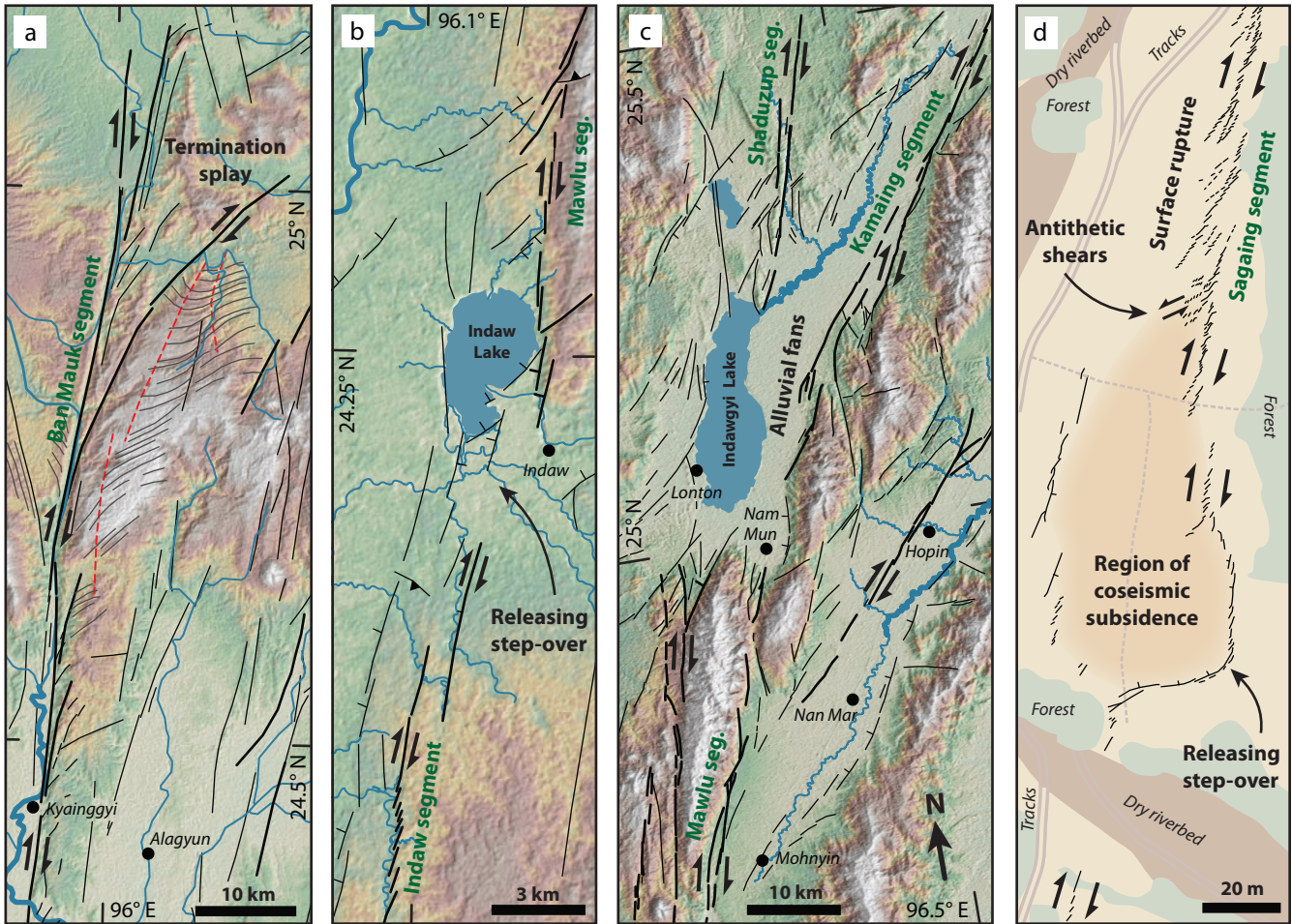


Fig. 19.8

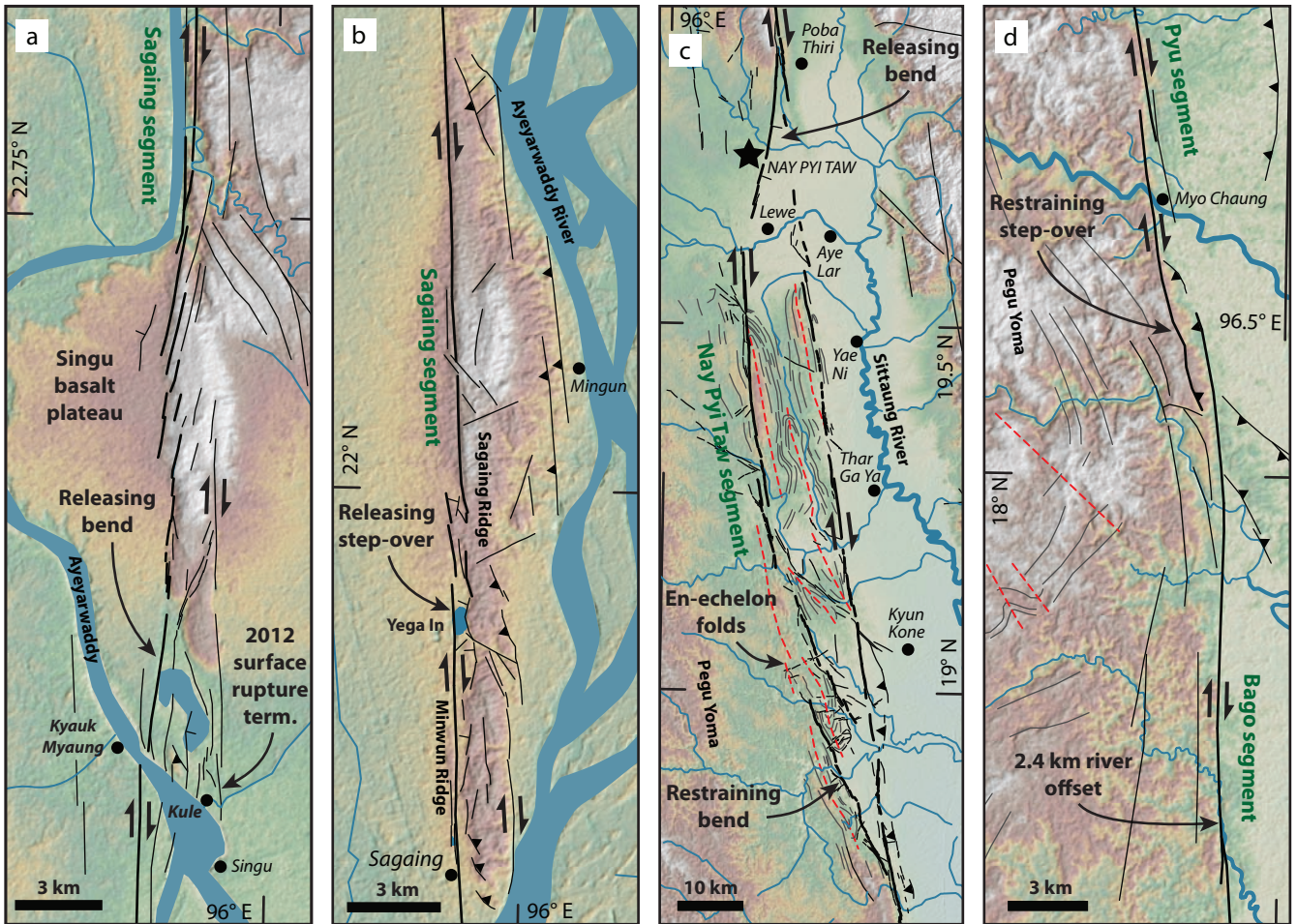


Fig. 9

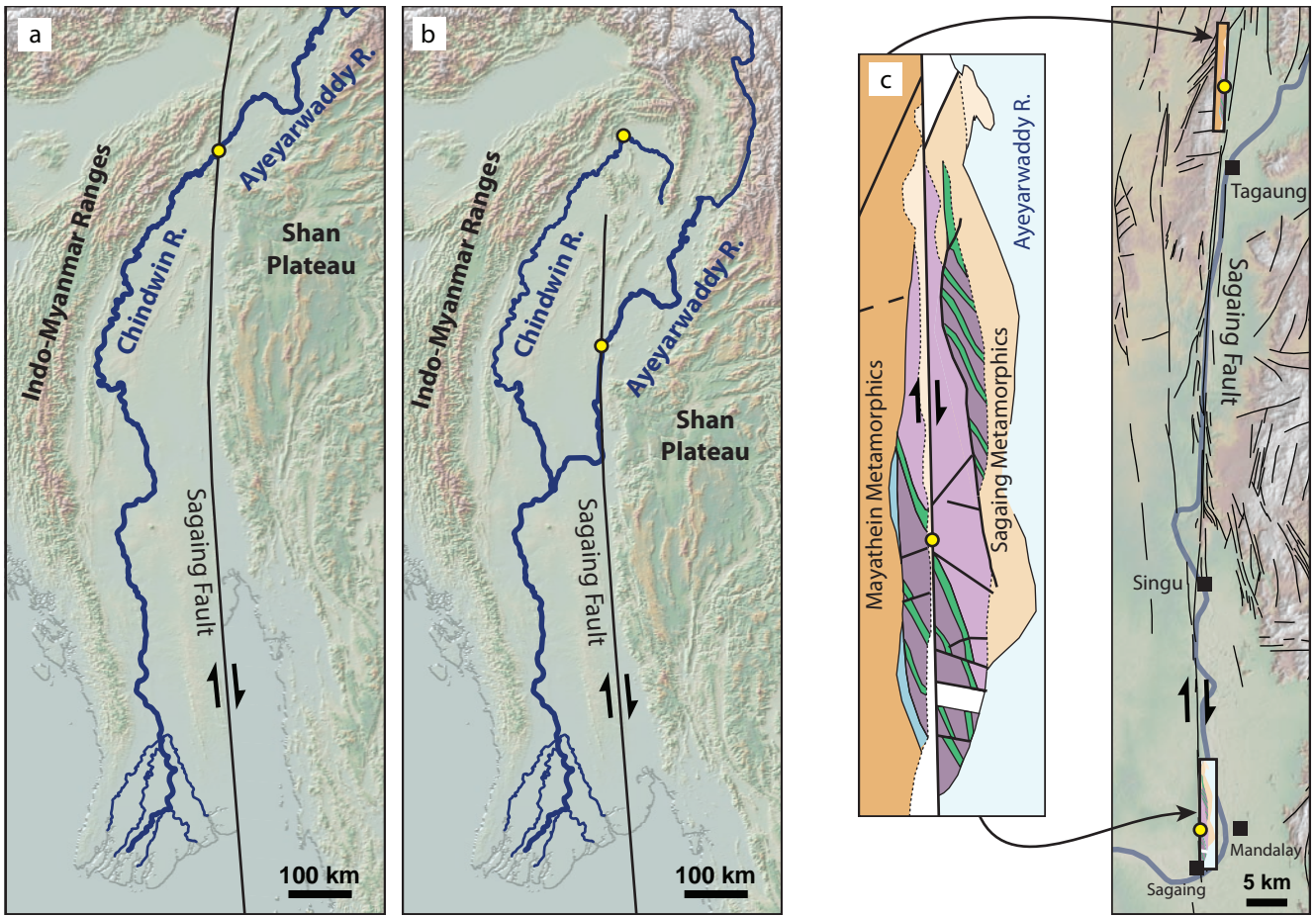


Fig. 19.10

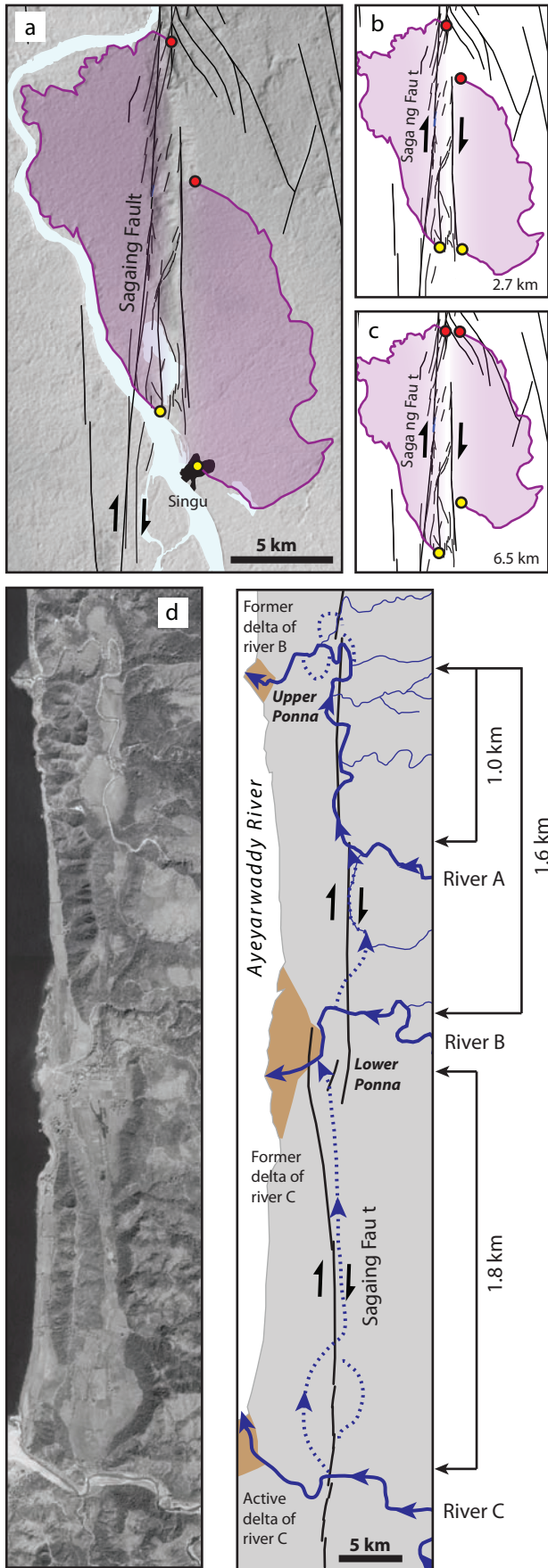


Fig. 19.11

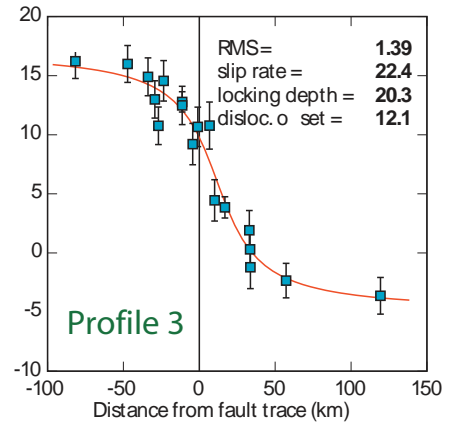
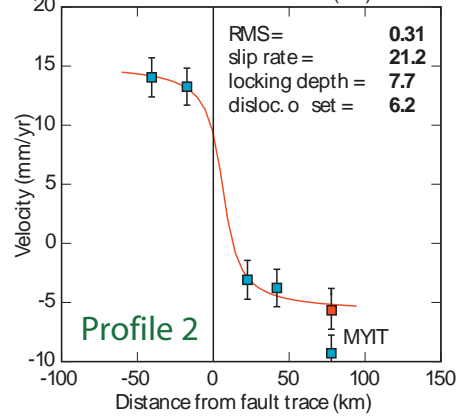
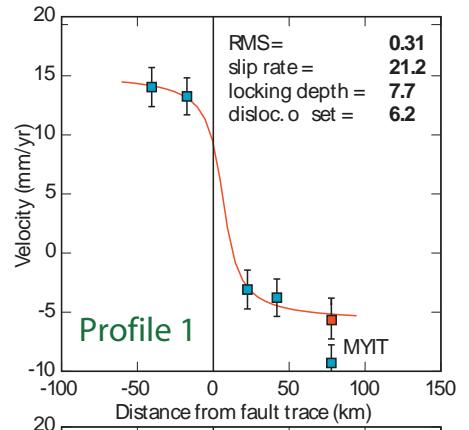
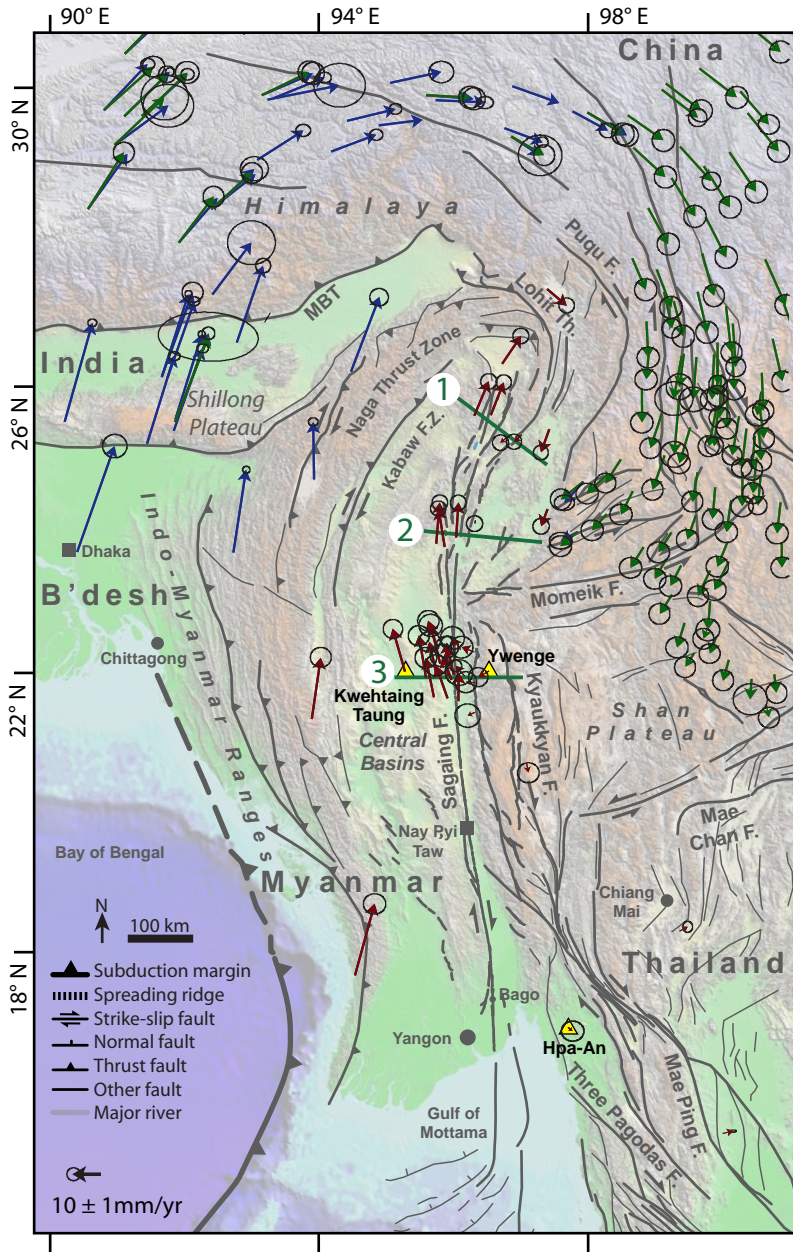


Fig. 19.12



Fig. 19.13

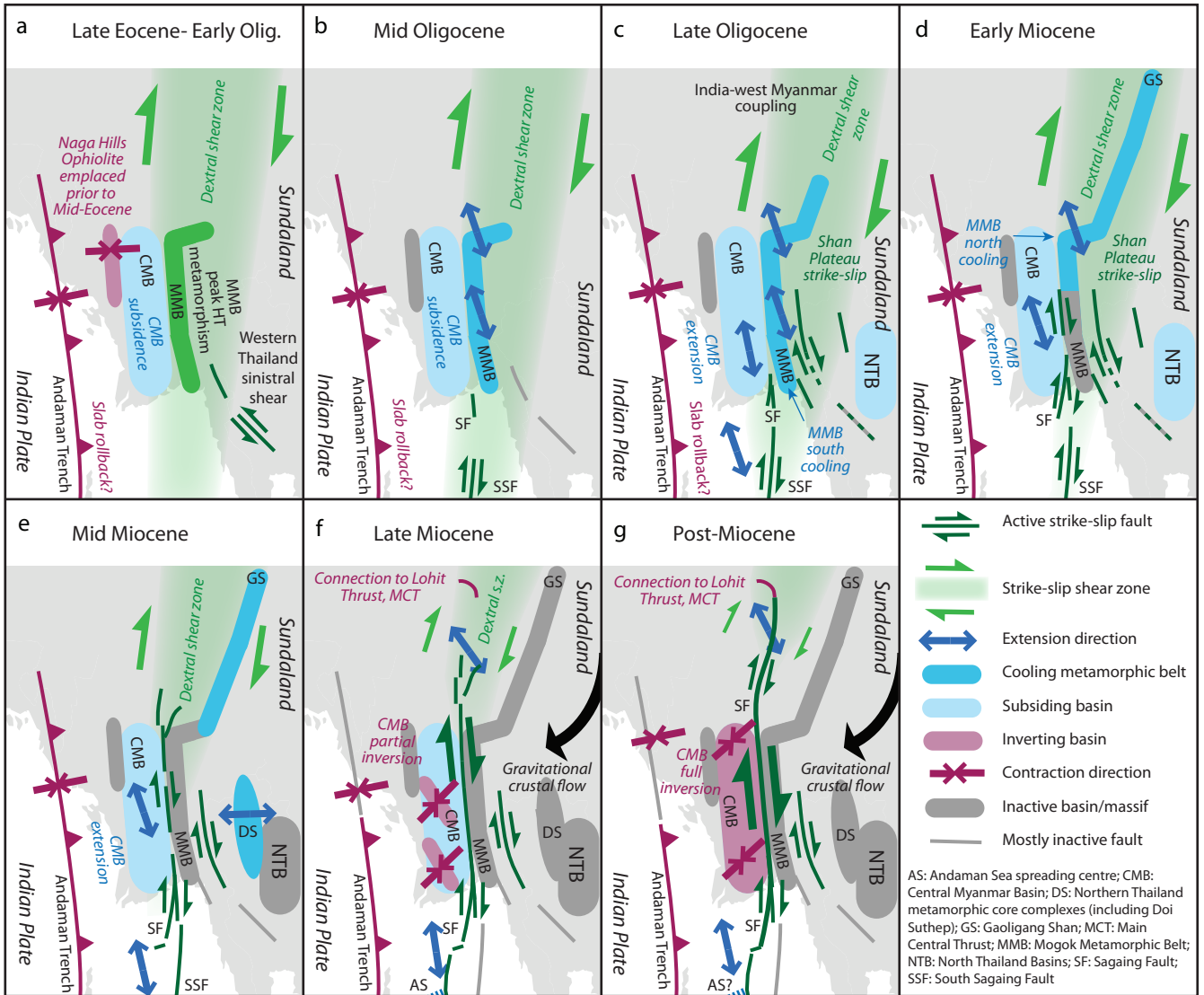


Fig. 19.14

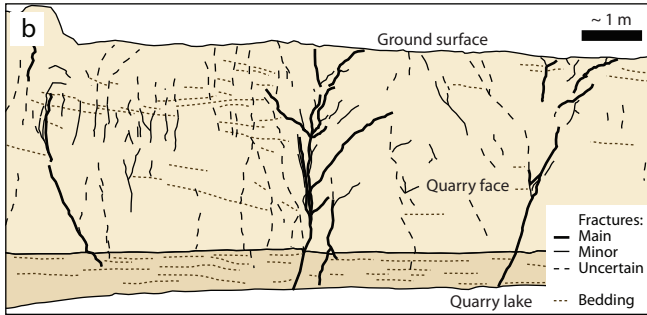
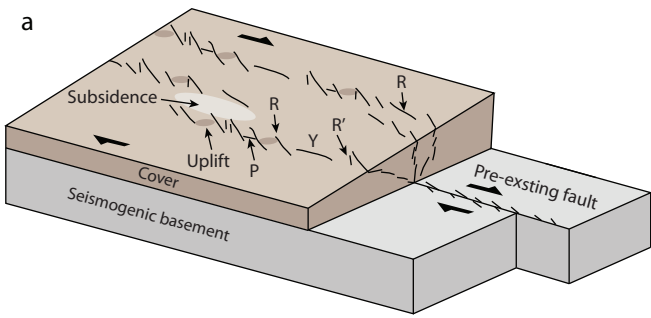


Fig. 19.15